



THE UNIVERSITY *of* EDINBURGH

## Edinburgh Research Explorer

# Mixed gas diffusion and permeation of ternary and quaternary CO<sub>2</sub>/ CO/ N<sub>2</sub>/O<sub>2</sub> gas mixtures in Matrimid®, polyetherimide and poly(lactic acid) membranes for CO<sub>2</sub>/CO separation

### Citation for published version:

Checchetto, R, Scarpa, M, De Angelis, G & Minelli, M 2022, 'Mixed gas diffusion and permeation of ternary and quaternary CO<sub>2</sub>/ CO/ N<sub>2</sub>/O<sub>2</sub> gas mixtures in Matrimid®, polyetherimide and poly(lactic acid) membranes for CO<sub>2</sub>/CO separation', *Journal of Membrane Science*, vol. 659, 120768.

### Link:

[Link to publication record in Edinburgh Research Explorer](#)

### Document Version:

Peer reviewed version

### Published In:

Journal of Membrane Science

### General rights

Copyright for the publications made accessible via the Edinburgh Research Explorer is retained by the author(s) and / or other copyright owners and it is a condition of accessing these publications that users recognise and abide by the legal requirements associated with these rights.

### Take down policy

The University of Edinburgh has made every reasonable effort to ensure that Edinburgh Research Explorer content complies with UK legislation. If you believe that the public display of this file breaches copyright please contact [openaccess@ed.ac.uk](mailto:openaccess@ed.ac.uk) providing details, and we will remove access to the work immediately and investigate your claim.



# Journal Pre-proof

Mixed gas diffusion and permeation of ternary and quaternary CO<sub>2</sub>/CO/N<sub>2</sub>/O<sub>2</sub> gas mixtures in Matrimid®, polyetherimide and poly(lactic acid) membranes for CO<sub>2</sub>/CO separation

R. Checchetto, M. Scarpa, M.G. De Angelis, M. Minelli

PII: S0376-7388(22)00513-0

DOI: <https://doi.org/10.1016/j.memsci.2022.120768>

Reference: MEMSCI 120768

To appear in: *Journal of Membrane Science*

Received Date: 12 May 2022

Revised Date: 15 June 2022

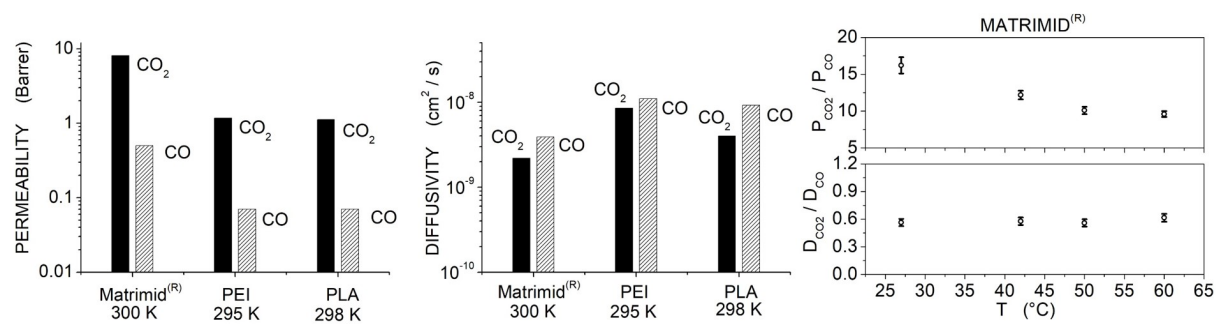
Accepted Date: 21 June 2022

Please cite this article as: R. Checchetto, M. Scarpa, M.G. De Angelis, M. Minelli, Mixed gas diffusion and permeation of ternary and quaternary CO<sub>2</sub>/CO/N<sub>2</sub>/O<sub>2</sub> gas mixtures in Matrimid®, polyetherimide and poly(lactic acid) membranes for CO<sub>2</sub>/CO separation, *Journal of Membrane Science* (2022), doi: <https://doi.org/10.1016/j.memsci.2022.120768>.

This is a PDF file of an article that has undergone enhancements after acceptance, such as the addition of a cover page and metadata, and formatting for readability, but it is not yet the definitive version of record. This version will undergo additional copyediting, typesetting and review before it is published in its final form, but we are providing this version to give early visibility of the article. Please note that, during the production process, errors may be discovered which could affect the content, and all legal disclaimers that apply to the journal pertain.

© 2022 Published by Elsevier B.V.



Matrimid<sup>(R)</sup>, PEI and PLA membranes for CO<sub>2</sub> / CO separation

1 **Mixed gas diffusion and permeation of ternary and quaternary**  
2  **$CO_2/CO/N_2/O_2$  gas mixtures in Matrimid<sup>®</sup>, polyetherimide and poly(lactic acid)**  
3 **membranes for  $CO_2/CO$  separation**  
4

5 R. Checchetto<sup>(1,\*)</sup>, M. Scarpa<sup>(1)</sup>, M.G. De Angelis <sup>(2)</sup>, M. Minelli<sup>(3)</sup>

6 <sup>(1)</sup> Dipartimento di Fisica - Università di Trento, Via Sommarive 14, I-28132 Povo (TN), Italy

7 <sup>(2)</sup> School of Engineering, University of Edinburgh, Sanderson Building, EH93FB, Edinburgh, UK

8 <sup>(3)</sup> Department of Civil, Chemical, Environmental and Materials Engineering, Alma Mater Studiorum  
9 – University of Bologna, via Terracini 28, I-40131 Bologna, Italy

10 (\*) e-mail: [riccardo.checchetto@unitn.it](mailto:riccardo.checchetto@unitn.it) ; [grazia.deangelis@ed.ac.uk](mailto:grazia.deangelis@ed.ac.uk)  
11

12 **Abstract**

13 The  $CO_2/CO$  mixed-gas separation performance of a polyimide (Matrimid<sup>®</sup>), polyetherimide (PEI) and  
14 polylactic acid (PLA) membrane, were characterized in the presence of  $CO_2$ - rich ternary ( $CO_2/CO/O_2$ ) and  
15 quaternary ( $CO_2/CO/O_2/N_2$ ) feed gas mixtures mimicking the products of  $CO_2$  reforming conversion  
16 reactions. The membrane- based separation of this mixture is poorly characterized and original data were  
17 obtained in a novel mass spectrometric apparatus that permits to monitor the instantaneous permeate  
18 composition, thus allowing to evaluate both mixed gas diffusion and permeability coefficients of all gases.  
19  $CO_2$ ,  $CO$ ,  $O_2$  and  $N_2$  permeability and diffusivity in single gas tests were measured between 298 and 353 K  
20 up to 1 atm feed pressure and relevant activation energies were evaluated. At 298 K Matrimid<sup>®</sup> exhibits  $CO$   
21 permeability of  $0.50 \pm 0.03$  Barrer and an ideal  $CO_2/CO$  selectivity of  $16 \pm 1$ . PEI and PLA exhibit similar ideal  
22 selectivity values but lower  $CO$  transport rates. In all examined polymer films the  $CO_2/CO$  selectivity has  
23 absorption-selective character that favours the permeation of  $CO_2$ . The ideal  $CO_2/CO$  selectivity of all  
24 membrane samples decreases with temperature, reaching values of  $10 \pm 1$  at 335 K in Matrimid<sup>®</sup>. The  
25  $CO_2/CO$  selective performances of all examined membrane do not show markable variations exposing the  
26 membrane samples to  $CO_2$ - rich gas mixtures as feed gas. The upper bound correlation among selectivity and  
27 permeability for the  $CO_2/CO$  gas couple is here for the first time proposed.  
28  
29

30 **Keywords:**

31 Polymeric membranes;  $CO_2$  plasma reforming; Mixed gas permeation/diffusion at  
32 different temperatures;  $CO$  transport;  $CO_2/CO$  separation mechanism.

## 33 1. Introduction

34  $CO_2$  reforming by non-thermal plasma (NTP) conversion is an emerging technique for  $CO_2$   
35 recycling. A non-thermal plasma operates at room temperature and atmospheric pressure  
36 generating highly active molecular/atomic species and energetic electrons with 1 to 10 eV energy:  
37 when electrons with energy in this interval value collide with molecules, excite them and break  
38 chemical bonds.  $CO_2$  dissociation occurs by  $CO_2 \rightarrow CO + \frac{1}{2}O_2$  reaction and requires only 5.5 eV;  
39 dissociation proceeds via stepwise vibrational excitation that breaks the  $OC = O$  bond [1,2]. When  
40 driven by renewable energy, this innovative  $CO_2$  conversion process would be an important step  
41 towards a sustainable energy scenario: it allows, in fact,  $CO_2$  recycling with the simultaneous storage  
42 of the electricity produced by the renewable sources in form of chemical fuels offering a solar-to-  
43 fuel efficiency close to 23 % [1,2]. Its implementation requires anyway the upgrading of the resulting  
44 gas mixture by separation of the unconverted  $CO_2$  molecules from  $CO$  [1,2].

45 Compared to the commercial separation technologies of Swing Adsorption or Cryogenic  
46 Distillation, membrane processes are of particular interest offering low energy consumption, high  
47 sustainability and environmentally friendly character [3,4]. Gas transport through a polymeric  
48 membrane occurs when a pressure difference is applied between the membrane opposite sides:  
49 the gas mixture components are separated because different gas species permeate through the  
50 membrane layers at different rates depending on their solubility and diffusivity in the polymeric  
51 layers [4]. There is very little knowledge on the  $CO$  transport properties and  $CO_2/CO$  separation  
52 performances of commercial polymeric gas separation membranes. Such information would be of  
53 importance not only for  $CO$  separation from mixtures produced by  $CO_2$  reforming, but also for  
54 separation of mixtures produced in processes such as partial oxidation of carbon- containing  
55 materials (coal and biomasses) or by steam reforming of natural gas [5].

56 In this work we present a detailed study on the  $CO$  transport properties and  $CO_2/CO$   
57 separation performances in multicomponent state of polymeric membranes exposed to  $CO_2$ - rich  
58 gas mixtures having composition similar to those produced by  $CO_2$  reforming by NTP conversion.  
59 The tests were carried out with a novel experimental mass spectrometric apparatus which allows to  
60 monitor the transient and steady-state multicomponent transport of gas mixtures in polymeric  
61 membranes with high accuracy, allowing to determine the mixed gas diffusion and permeation  
62 coefficients, which are extremely rare and time-consuming, as recent studies reveal [6]. Tests were  
63 carried out using dense Matrimid<sup>®</sup>, polyetherimide (PEI) and polylactic acid (PLA) membrane films.  
64 Matrimid<sup>®</sup> is an aromatic polyimide with glassy structure exhibiting high thermal stability ( $T_g =$

65 302°C) and acceptable values of selectivity and permeability for  $CO_2/CH_4$  separation and  $H_2$   
66 purification applications [7]. PEI is an amorphous thermoplastic with glass transition temperature  
67 at 217°C, decomposition temperature at 427°C and 1.27 g/cm<sup>3</sup> density offering excellent chemical  
68 resistance and high strength [8]. PLA is a “green” innovative aliphatic polyester having 1.24 g/cm<sup>3</sup>  
69 density and 160°C melting point that is produced from the fermentation of renewable resources  
70 such as crops studied for packaging applications as substitute of commercial petroleum- derived  
71 polymers [9]. Matrimid® and PEI were chosen for this study because these commercial polymers are  
72 used for the construction of hollow fiber membranes employed in industrial plants for biogas  
73 upgrading [10,11] and it is thus of interest a study on their  $CO_2/CO$  separation properties. PLA was  
74 chosen because the transport properties of various gases in this biopolymer are of interest for its  
75 envisaged applications [9] and no information is currently present regarding the  $CO$  permeation  
76 process.

77 The aim of this paper is to present original data on the  $CO$  permeability and diffusivity in the  
78 examined polymer samples and analyze their  $CO_2/CO$  selective properties at different  
79 temperatures. Separate information on gas permeability and diffusivity in the examined samples  
80 will be presented to underline the mechanism responsible of the membrane separation properties.  
81 Permeation tests were carried out in single gas and in mixed gas conditions: the comparison  
82 between single gas transport and gas mixture transport is of great importance because when the  
83 membrane is exposed to gas mixtures, as it occurs in real operative conditions, microscopic  
84 phenomena such as competitive sorption effects, plasticization processes and matrix dilation affect  
85 the transport of gas mixture components and the membrane selectivity values can thus differ from  
86 the ideal ones [12].

87

## 88 2. Experimental

### 89 2.1 Materials

90 Matrimid® films with thickness of  $60 \pm 2 \mu\text{m}$  were prepared dissolving polyimide powders  
91 (kindly provided by Huntsman Advanced Materials) in dichloromethane (Sigma-Aldrich) (1.5 wt. %)  
92 and the resulting solution was casted in a petri dish; after solvent evaporation in a clean hood  
93 overnight, the resulting film was inserted in a vacuum oven at 200°C overnight.

94 Polyetherimide (PEI) films with thickness of  $80 \pm 2 \mu\text{m}$  were prepared dissolving 0.65 g  
95 polyetherimide pellets with density 1.27 g/cm<sup>3</sup> (Sigma-Aldrich, Milan) in 40 mL  $CHCl_3$ . The solution  
96 was heated to about 40-50°C and kept under stirring until complete dissolution. Then it was casted

97 on glass dishes, dried at RT for 5 days, then in an oven at 60°C for 24 h and finally in a desiccator  
 98 under mild vacuum until utilization.

99 Nearly amorphous PLA films with thickness of  $50 \pm 2 \mu\text{m}$  were prepared dissolving PLA pellets  
 100 (Nature Works LLC, PLA 4032D) in chloroform (1 g PLA / 25 ml  $\text{CHCl}_3$ ) at 40°C under magnetic stirring  
 101 until completely dissolved. Film samples were obtained casting the resulting solution in a petri dish;  
 102 the solvent was let evaporate first at room temperature for 24 hours and then for 4 hours in a  
 103 ventilated oven at 40° C. DSC analysis not reported here revealed that the crystalline content of the  
 104 present film samples was lower than 3 %.

105 We studied the transport of carbon dioxide ( $\text{CO}_2$ ), carbon monoxide ( $\text{CO}$ ), nitrogen ( $\text{N}_2$ ),  
 106 synthetic air (a dry mixture of 20 vol. %  $\text{O}_2$  and 80 vol. %  $\text{N}_2$ ) and of two gas mixtures, M224 and  
 107 M225, whose composition is reported in Table I. These mixtures were prepared by a static method  
 108 introducing known amounts of single gas components into a previously evacuated rigid vessel; their  
 109 composition mimics that of mixtures resulting from  $\text{CO}_2$  plasma reforming [13,14].  
 110

	$\text{CO}_2$ (vol %)	$\text{CO}$ (vol %)	$\text{O}_2$ (vol %)	$\text{N}_2$ (vol %)
M224	$64 \pm 1$	$26 \pm 1$	$9 \pm 1$	-
M225	$30 \pm 1$	$26 \pm 1$	$9 \pm 1$	$34 \pm 1$

111 Table I: Composition of the ternary (M224) and quaternary (M225) gas mixtures.  
 112

113 The molecular diameters ( $\sigma_k$ ) and critical temperatures ( $T_c$ ) of test gases are reported in  
 114 Table II [15]. Gas transport tests were carried out at temperature and feed pressure values relevant  
 115 for  $\text{CO}_2$  plasma reforming processes, namely  $T < 100^\circ\text{C}$  and  $p_{feed} < 10^5 \text{ Pa}$ .  
 116  
 117

gas	$\sigma_k$ (pm)	$\sigma_{LJ}$ (pm)	$\sigma_C$ (pm)	$V_c$ ( $\text{cm}^3/\text{mol}$ )	$T_c$ (K)	$\gamma_\alpha$ (A/Pa)	$s_p$ ( $\text{m}^3/\text{s}$ )
$\text{CO}_2$	330	394	365	91.9	304.19	$6.71 \times 10^{-3}$	$130 \pm 2$
$\text{CO}$	376	369	363	90.1	132.91	$5.91 \times 10^{-3}$	$140 \pm 2$
$\text{N}_2$	364	380	361	89.4	126.2	$5.63 \times 10^{-3}$	$125 \pm 2$
$\text{O}_2$	346	345	339	73.5	154.6	$4.54 \times 10^{-3}$	$135 \pm 2$

118 Table II: Kinetic diameters ( $\sigma_k$ ), Lennard-Jones diameters ( $\sigma_{LJ}$ ), Chung diameter ( $\sigma_C$ ), critical molar volume  
 119 ( $V_c$ ) and temperatures ( $T_c$ ) of the examined test gases [15]. The last two columns report the QMS sensitivity  
 120  $\gamma_\alpha$  and the pumping speed of our vacuum system for each gas specie. Values of the  $\beta$  parameters are:  
 121  $\beta(\text{CO}^+/\text{CO}_2) = 0.099$  and  $\beta(\text{N}^+/\text{N}_2) = 0.103$ . Experimental indetermination of the  $\gamma_\alpha$  and  $\beta$  parameters is  
 122  $\sim 1\%$  [16].  
 123  
 124

## 125 2.2 Gas transport tests

126 The description of the experimental apparatus and of the procedure for the analysis of the  
 127 gas mixture transport kinetics through polymeric membranes is reported in a previous paper [16].  
 128 Permeation tests were carried out by gas-phase permeation technique in dead-end configuration.  
 129 At time  $t = 0$  the feed side of the membrane sample is exposed to the feed gas at total pressure  
 130  $p_{feed} = \sum_{\alpha} p_{feed}^{\alpha}$ ; in the previous relation  $p_{feed}^{\alpha}$  is the partial pressure value of the gas specie  $\alpha$ .  
 131 Penetrant molecules permeate through the membrane in a vacuum chamber of volume  $V$  and  
 132 temperature  $T_{ch}$ ; these molecules form in this volume a gas mixture having total pressure  $p(t) =$   
 133  $\sum_{\alpha} p_{\alpha}(t)$ . The partial pressure of the permeated  $\alpha$  molecules,  $p_{\alpha}(t)$ , changes with time  $t$  according  
 134 to the relation:

$$135 \quad \frac{1}{R T_{ch}} \left[ V \frac{dp_{\alpha}(t)}{dt} + s_p p_{\alpha}(t) \right] = A j_{\alpha}(t) \quad (1)$$

136 where  $R$  is the universal gas constant,  $s_p$  the effective pumping speed of the vacuum system. In the  
 137 previous relation  $j_{\alpha}(t)$  is the permeation flux of the  $\alpha$  gas specie and  $A$  the membrane surface area.  
 138 Tests were carried out with the analysis chamber under dynamic pumping conditions using a  
 139 vacuum system based on turbo-molecular pumps [16]. When the condition  $\frac{s_p}{V} \gg \frac{1}{p_{\alpha}(t)} \frac{dp_{\alpha}(t)}{dt}$  is  
 140 satisfied then  $p_{\alpha}(t)$  is a measure of the permeation flux  $j_{\alpha}(t)$  of the  $\alpha$  gas specie by the relation:

$$141 \quad j_{\alpha}(t) = \frac{1}{A} \frac{1}{R T_{ch}} s_p p_{\alpha}(t) \quad (2)$$

142 In our experimental approach we measured  $p_{\alpha}(t)$  as a function of time  $t$  with a calibrated  
 143 Quadrupole Mass Spectrometer (QMS) equipped with a grid- type ion source and a 90° off-axis  
 144 Secondary Electron Multiplier (SEM) for ion detection.

145 This instrument was calibrated by the following procedure [16]. We injected pure gas  $\alpha$  in  
 146 the continuously pumped permeation chamber through a variable leak valve and recorded the  
 147  $i(\alpha^+/\alpha)$  and  $i(\alpha_i^+/\alpha)$  QMS ion currents pertinent to the singly charged molecular ion ( $\alpha^+/\alpha$ ) and  
 148 its fragmentation ions ( $\alpha_i^+/\alpha$ ). After background subtraction, the QMS sensitivity  $\gamma_{\alpha}$  for the test  
 149 gas  $\alpha$  was obtained as:

$$150 \quad \gamma_{\alpha} = \frac{i(\alpha^+/\alpha)}{p_{\alpha}} \quad (3)$$

151 while the QMS sensitivity for the ( $\alpha_i^+/\alpha$ ) fragmentation ion relative to that of the ( $\alpha^+/\alpha$ ) ion by  
 152 the relation:

$$153 \quad \beta(\alpha_i^+/\alpha) = \frac{i(\alpha_i^+/\alpha)}{i(\alpha^+/\alpha)} \quad (4)$$

154 Values of the  $\gamma_{\alpha}$ ,  $\beta(\alpha_i^+/\alpha)$  and of the  $s_p$  parameters are reported in Table II. Calibration procedures  
 155 and pertinent validation tests are presented in ref. [16].

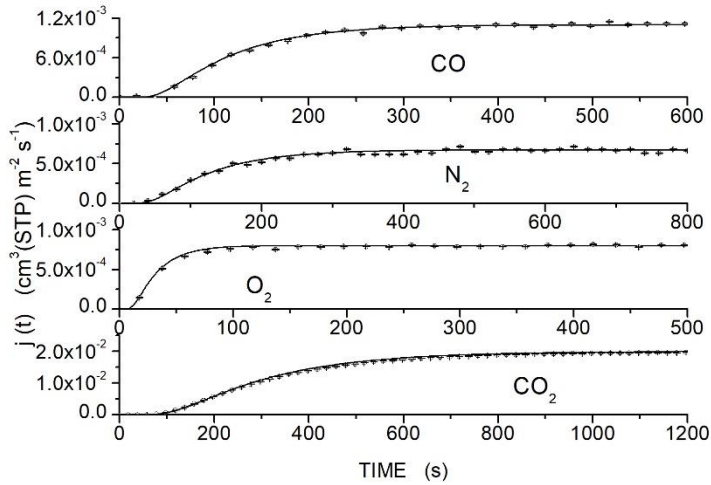


156 In single gas tests we exposed the membrane samples to the  $\alpha$  gas specie and recorded the  
 157  $i(\alpha^+/\alpha)$  ion current which represents the net mass signal  $s_\alpha(t)$ ; the partial pressure  $p_\alpha(t)$  in the  
 158 permeation chamber of this gas specie was then evaluated by eq. 3 and the permeation flux  
 159 transient  $j_\alpha(t)$  by eq. 2. As an example in fig. SI1 we report the  $s_\alpha(t)$  signals obtained with the PLA  
 160 membrane films while in fig. 1 we report the corresponding  $j_\alpha(t)$  curves obtained converting  
 161 sampled  $s_\alpha(t)$  data by eq. 2 using parameters in Table II.

162

163 In mixed gas tests we recorded, for each  $\alpha$  gas specie forming the feed mixture, the pertinent  
 164  $i(\alpha^+/\alpha)$  and  $i(\alpha_i^+/\alpha)$  ion currents. The net mass signal,  $s_\alpha(t)$ , was then obtained as follows. The  
 165  $s_{CO_2}(t)$  and  $s_{O_2}(t)$  signals are unambiguously given by the  $i(CO_2^+/CO_2)$  and  $i(O_2^+/O_2)$  QMS ion  
 166 currents having mass-charge ratio  $m/e = 44$  and  $32 Da$ , respectively. The  $s_{N_2}(t)$  signal was  
 167 obtained monitoring the  $s_N(t) = i(N^+/N_2)$  ion current ( $m/e = 14 Da$ ) resulting from the  $N^+$  ions  
 168 formed in the electron- impact fragmentation of the  $N_2$  molecules:  $s_{N_2}(t) = s_N(t)/\beta(N^+/N_2)$ . In  
 169 our experimental mixed gas tests, the  $i(m/e = 28 Da)$  ion current is given by three contributions:  
 170 the contribution of the  $(CO^+/CO)$  ions formed in the ionization of the carbon monoxide molecule,  
 171 the contribution of the  $(CO^+/CO_2)$  ions formed upon electron- impact fragmentation of  $CO_2$   
 172 molecules and the contribution from the  $(N_2^+/N_2)$  ions. The net  $CO$  mass signal,  $s_{CO}(t)$ , was  
 173 obtained subtracting the signal  $\varphi_{CO} = \beta(CO^+/CO_2) i(CO_2^+/CO_2) + s_N(t)/\beta(N^+/N_2)$  from the  
 174  $i(m/e = 28 Da)$  ion current:  $s_{CO}(t) = i(m/e = 28 Da) - \varphi_{CO}$  [16]. As examples to illustrate the  
 175 procedure, in the Supplementary Information Section, we report in figs. SI2 and SI3 the  $s_\alpha(t)$  signals  
 176 obtained in permeation tests exposing the PEI membrane to the M224 gas mixture at  $T = 300 \pm 2$   
 177 K (fig. SI2) and the Matrimid® membrane film to the M225 gas mixture at  $T = 300 \pm 2$  K (fig. SI3).  
 178 The partial pressure  $p_\alpha(t)$  in the permeation chamber of each gas specie forming the gas mixture  
 179 was then evaluated by eq. 3 and its permeation flux transient  $j_\alpha(t)$  by eq. 2. Figs. 2 and 3 report as  
 180 symbols the  $j_\alpha(t)$  permeation curves obtained using sampled  $s_\alpha(t)$  data of fig. SI2 and SI3.

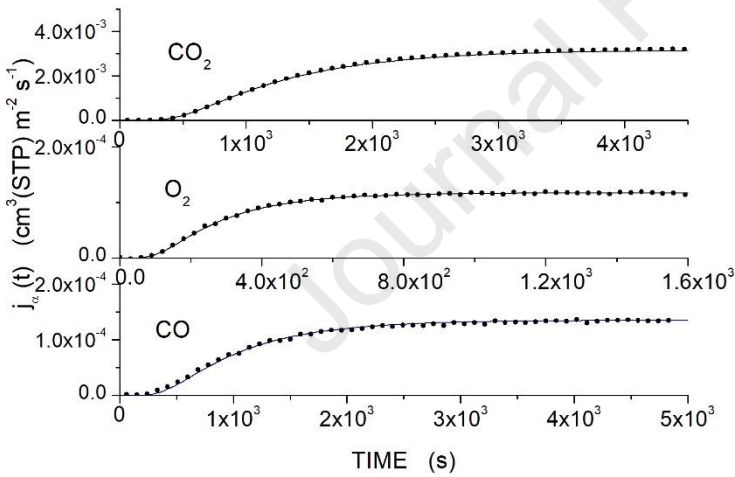
181



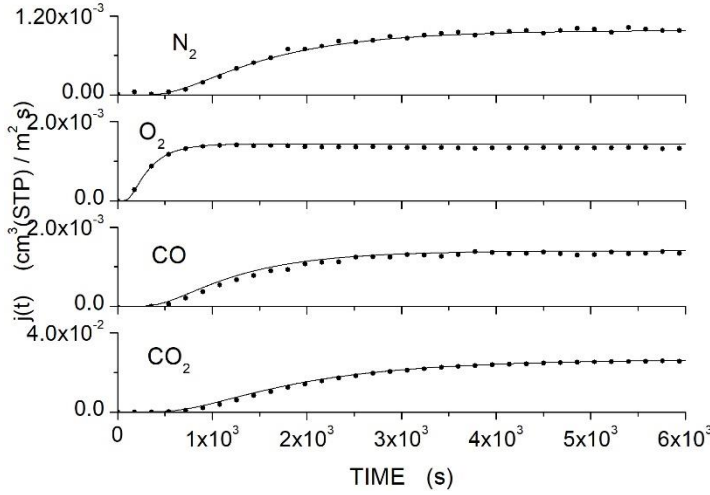
182  
 183 Fig. 1:  $j_{\alpha}(t)$  permeation curves obtained with the PLA membrane samples exposed to pure gases  $CO_2$ ,  $CO$   
 184 and  $N_2$  gas ( $p_{feed} = 45 \pm 1$  kPa) and to the dry  $N_2/O_2$  gas mixture ( $p_{feed} = 72 \pm 1$  kPa) at  $T = 298 \pm 2$  K.  
 185 Curves were calculated converting sampled  $s_{\alpha}(t)$  data of fig. SI1 by eq. 2.  
 186

187

188



189  
 190 Fig. 2:  $j_{\alpha}(t)$  permeation curves obtained with the PEI membrane samples exposed to the M224 gas mixture  
 191 ( $p_{feed} = 45 \pm 1$  kPa) at  $T = 295 \pm 2$  K. Curves were calculated converting sampled  $s_{\alpha}(t)$  data of fig. SI2 by  
 192 eq. 2.  
 193



194

195 Fig. 3:  $j_\alpha(t)$  permeation curves obtained with the Matrimid® membrane samples exposed to the M225 gas  
 196 mixture ( $p_{feed} = 72 \pm 1$  kPa) at  $T = 300 \pm 2$  K. Curves were calculated converting sampled  $s_\alpha(t)$  data of fig.  
 197 SI3 by eq. 2.

198

199

### 200 3. Results and discussion

#### 201 3.1 Data analysis

202 The experimental  $j_\alpha(t)$  permeation curves, as obtained in single and mixed gas conditions,  
 203 were analysed assuming that the permeation process obeys to the solution-diffusion mechanism  
 204 [17]. According to this mechanism, when the feed side of a homogeneous membrane of thickness  $L$   
 205 is exposed at time  $t = 0$  to the feed gas at pressure  $p_{feed}^\alpha$ , the gas molecules are absorbed in the  
 206 membrane surface layers and their concentration here,  $c_\alpha$ , immediately reaches the equilibrium  
 207 value given  $c_\alpha = S_\alpha p_{feed}^\alpha$  where  $S_\alpha$  is the gas solubility in the polymeric membrane at interfacial  
 208 conditions. In glassy polymers  $S_\alpha$  can be described by the dual-mode sorption [18].

209 Absorbed molecule diffuse through the membrane layers to the opposite side down to their  
 210 concentration gradient according to the Fick's law and are here desorbed [17]. The kinetics of the  
 211 permeation process is described by the following relationship [19], valid for a constant diffusion  
 212 coefficient:

$$213 \quad f_\alpha(t) = F_\alpha \left[ 1 + 2 \sum_{n \geq 1} (-1)^n e^{-\frac{D_\alpha n^2 \pi^2 t}{L^2}} \right] \quad (5)$$

$$214 \quad F_\alpha = \frac{D_\alpha}{L} S_\alpha p_{feed}^\alpha = \frac{P_\alpha}{L} p_{feed}^\alpha \quad (6)$$

215 in which  $f_\alpha(t)$  is the permeation flux as a function of time  $t$  (flux transient),  $D_\alpha$  is the gas diffusivity  
 216 in the membrane layers and  $F_\alpha$  the permeation flux of the  $\alpha$  gas specie in stationary transport  
 217 conditions. The parameter  $P_\alpha = D_\alpha S_\alpha$  is the membrane gas permeability.

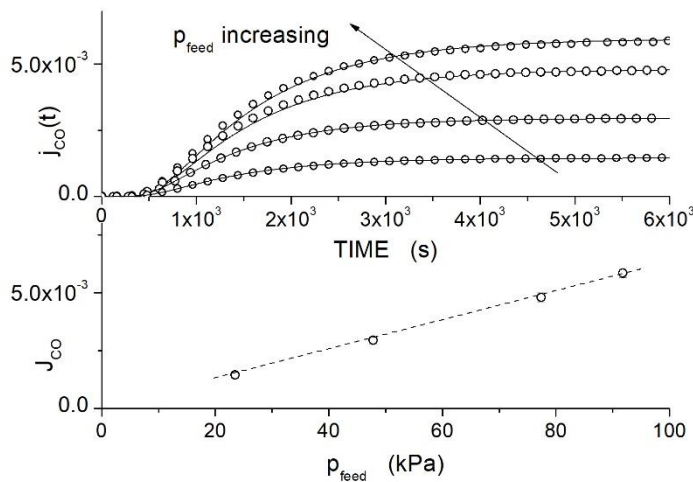
218 This approach permits to evaluate separately the penetrant permeability and diffusivity. The values  
 219 of the  $P_\alpha$  and  $D_\alpha$  transport parameters were, in fact, obtained as follows:  $P_\alpha$  was calculated  
 220 measuring the permeation flux of the  $\alpha$  gas specie in stationary transport conditions,  $J_\alpha$ , and using  
 221 eq. 6 while the  $D_\alpha$  value by best fitting the experimental  $j_\alpha(t)$  curves by eq. 5. In single-gas  
 222 conditions the  $p_{feed}^\alpha$  value in eq. 5 is the total pressure of the feed gas while in mixed gas conditions  
 223 (and with synthetic air)  $p_{feed}^\alpha$  is the partial pressure of the  $\alpha$  gas specie in the feed mixture ( $p_{feed} =$   
 224  $\sum_\alpha p_{feed}^\alpha$ ).

225

### 226 3.2 Permeation tests

227 In the upper panel of fig. 4 we present, as an example, the  $j_{CO}(t)$  permeation curves  
 228 obtained at  $T = 295$  K in single gas tests exposing the Matrimid® membrane sample to carbon  
 229 monoxide ( $CO$ ) at different feed pressure values. In the lower panel of this figure the value of  $j_{CO}(t)$   
 230 flux in stationary transport conditions ( $J_{CO}$ ) is reported as a function of the  $CO$  feed pressure,  $p_{feed}^{CO}$ .  
 231 The linear relationship between  $J_{CO}$  and  $p_{feed}^{CO}$  evidences that in this pressure interval the  $CO$   
 232 transport through the Matrimid® membrane film has a constant permeability coefficient, as  
 233 reasonable due to the low-pressure range inspected: similar trend was observed also with the PEI  
 234 and PLA membranes. From similar sets of permeation curves, the  $P_\alpha$  and  $D_\alpha$  values were evaluated  
 235 as average value of the permeability and diffusivity values obtained in each test while their  
 236 uncertainty as values semi-dispersion.

237



238 Fig. 4: Upper panel:  $j_{CO}(t)$  curves obtained at  $T = 300$  K in single gas tests exposing the Matrimid®  
 239 membrane sample to carbon monoxide at different feed pressure values [units:  $\text{cm}^3(\text{STP}) / \text{m}^2 \text{ s}$ ]. Lower  
 240 panel: value of the  $j_{CO}(t)$  flux in stationary transport conditions ( $J_{CO}$ ) as a function of the  $CO$  feed pressure  
 241 [units of  $J_{CO}$ :  $\text{cm}^3(\text{STP}) / \text{m}^2 \text{ s}$ ].  
 242

243

244 The Arrhenius plot of the  $P_\alpha$  and  $D_\alpha$  values obtained in single gas permeation tests is  
 245 reported in the left panel of fig. 5 for Matrimid<sup>®</sup>, of fig. 6 for PEI and of fig. 7 for PLA; the right panels  
 246 report data obtained exposing the membrane samples to the M224 gas mixture. The gas solubility  
 247 values  $S_\alpha$  calculated by the relation  $S_\alpha = P_\alpha/D_\alpha$  using  $P_\alpha$  and  $D_\alpha$  data pertinent to single gas test  
 248 for the  $CO_2$  and  $CO$  penetrant molecules are reported in Fig. 8.

249 The numerical values of the gas transport parameters in figs. 5-8 can be found in the  
 250 Supplementary Information Sections together with data obtained with the M225 gas mixture, see  
 251 Tables. SI1-SI3.  $N_2$  diffusivity values in Matrimid<sup>®</sup> and PEI are equal, within the experimental  
 252 indetermination, to  $CO$  diffusivity values (see Tables. SI1 and SI2) and are thus not reported in the  
 253 right panels of figs. 5 and 6.

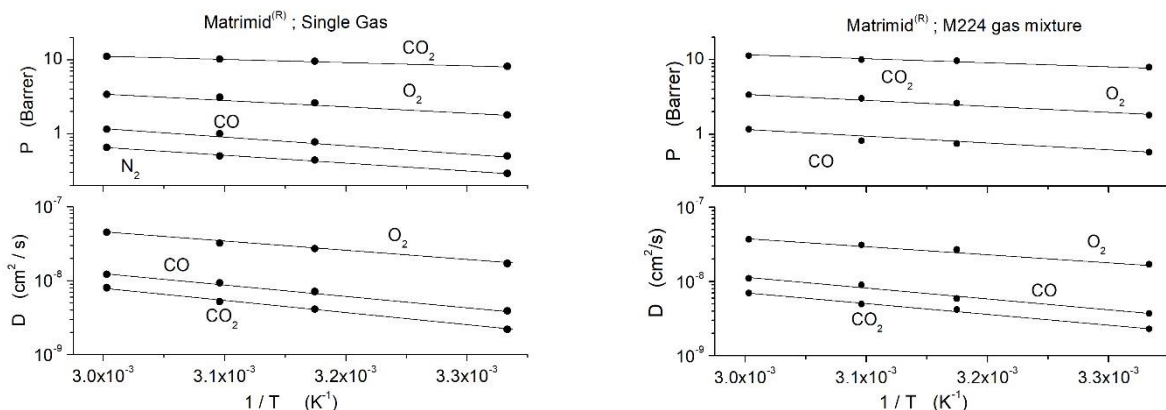
254 At each examined temperature, the following trend holds for the permeability coefficients:  
 255  $P_{CO_2} > P_{O_2} > P_{CO} \sim P_{N_2}$  and the following for the diffusion coefficients:  $D_{O_2} > D_{CO} \sim D_{N_2} > D_{CO_2}$ .

256 The experimental data evidence that the best correlation of diffusivity with penetrants'  
 257 molecular size is observed if the Lennard-Jones diameter  $\sigma_{LJ}$  is accounted for, rather than the  
 258 collisional diameter  $\sigma_K$ , see Table II and fig. SI4 [20].

259 We also observe that increasing temperature the permeability and diffusivity values  
 260 increase: such increase is nearly negligible for the glassy PEI film and results more marked for the  
 261 diffusivity than for the permeability values.

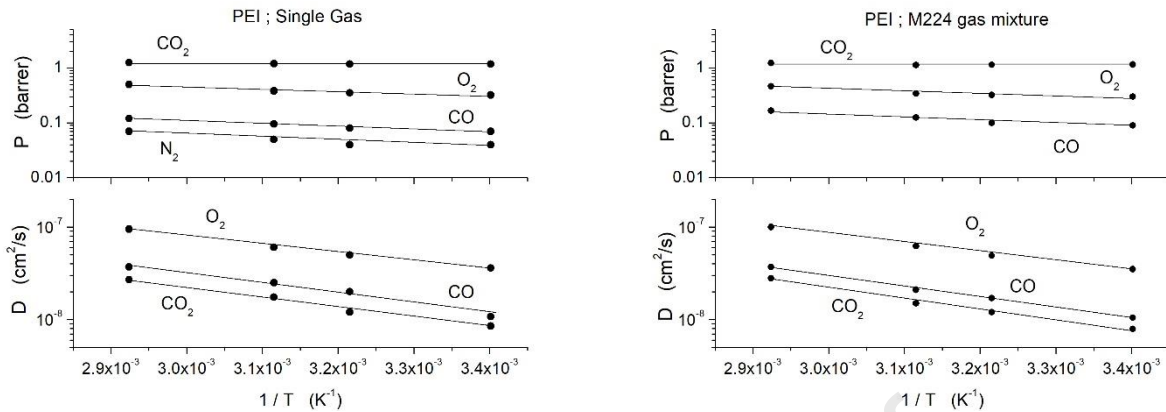
262

263



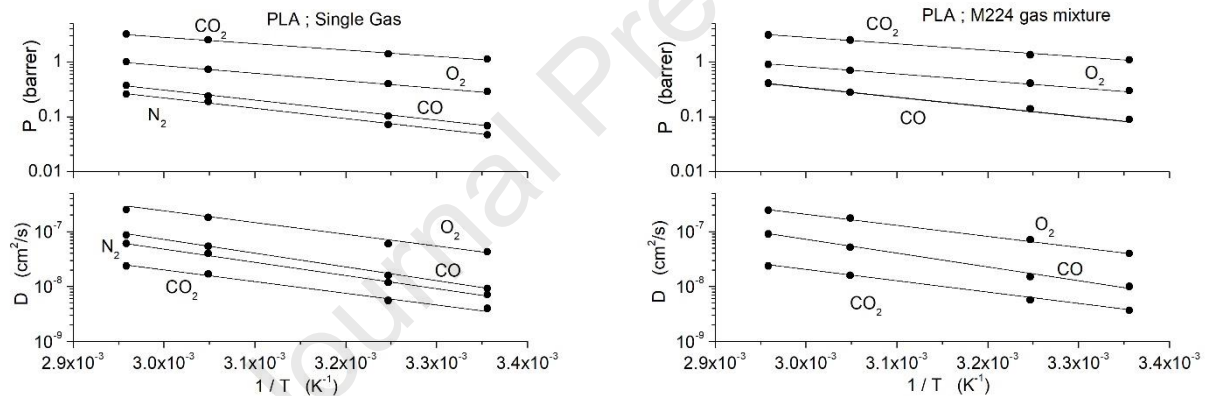
264 Fig. 5: Arrhenius plot of the gas permeability ( $P$ ) and diffusivity ( $D$ ) of the Matrimid<sup>®</sup> membrane sample as  
 265 obtained in single gas permeation tests (left panel) and with the ternary M224 gas mixture (right panel).  
 266 Numerical values are reported in the Supplementary Information section.  $N_2$  diffusivity values measured in  
 267 Single Gas conditions (left panel) are not reported as overlap with  $CO$  diffusivity values. Permeation tests  
 268 were carried out with feed pressure between 20 and 90 kPa.

269  
270



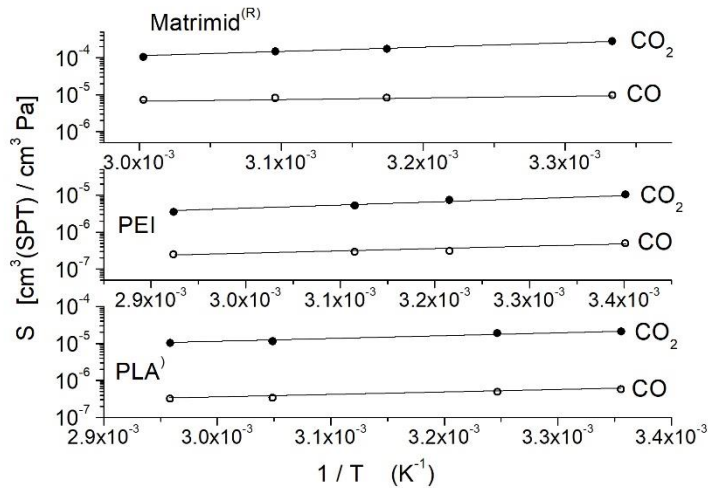
271 Fig. 6: Arrhenius plot of the gas permeability ( $P$ ) and diffusivity ( $D$ ) of the PEI membrane sample as obtained  
 272 in single gas permeation (left panel) and with the ternary M224 gas mixture (right panel). Numerical values  
 273 are reported in the Supplementary Information section.  $\text{N}_2$  diffusivity values measured in Single Gas  
 274 conditions (left panel) are not reported as overlap with  $\text{CO}$  diffusivity values. Permeation tests were carried  
 275 out with feed pressure between 20 and 90 kPa.

276  
277



278 Fig. 7: Arrhenius plot of the gas permeability ( $P$ ) and diffusivity ( $D$ ) of the PLA membrane film as obtained in  
 279 single gas permeation tests (left panel) and with the ternary M224 gas mixture (right panel). Numerical values  
 280 are reported in the Supplementary Information section. Permeation tests were carried out with feed  
 281 pressure between 20 and 90 kPa.

282  
283



284  
285 Fig. 8: Arrhenius plot of the gas solubility ( $S$ ) of the Matrimid<sup>®</sup>, PEI and PLA membrane film in single gas  
286 permeation tests obtained using  $P$  and  $D$  data in the left panels of figs. 4-6 by the relation  $S = P/D$ .  
287 Numerical values are reported in the Supplementary Information section. Permeation tests were carried out  
288 with feed pressure between 20 and 90 kPa.

289  
290

291

292 The activation energy values obtained by fitting permeability and diffusivity data in the left  
293 panels of figs. 5-7 by the Arrhenius equation are reported in Table III and IV, respectively.

294

$E_p$ (kJ/mol)	$CO_2$	$N_2$	$O_2$	$CO$
Matrimid <sup>®</sup>	$7.7 \pm 0.5$	$20.3 \pm 0.8$	$16 \pm 1$	$20.7 \pm 0.9$
PEI	$1.0 \pm 0.2$	$10 \pm 1$	$8 \pm 1$	$9.3 \pm 0.5$
PLA	$22.4 \pm 0.5$	$36.9 \pm 0.7$	$25.1 \pm 0.8$	$36 \pm 1$

295 Table III: Activation energy values for permeation obtained in single gas tests fitting  $P_\alpha$  data in in the left  
296 panels of Figs. 5-7.

297

298

$E_D$ (kJ/mol)	$CO_2$	$N_2$	$O_2$	$CO$
Matrimid <sup>®</sup>	$32.5 \pm 0.4$	$29.5 \pm 0.3$	$24.5 \pm 0.8$	$28.7 \pm 0.9$
PEI	$20.0 \pm 0.6$	$21.9 \pm 0.7$	$16.7 \pm 0.5$	$21.9 \pm 0.7$
PLA	$39 \pm 1$	$46 \pm 1$	$39 \pm 1$	$47 \pm 1$

299 Table IV: Activation energy values for diffusion obtained in single gas tests fitting  $D_\alpha$  data in the left panels  
300 of Figs. 5-7.

301

302

303 Because only few studies exist on the permeability of the  $CO$  penetrant in polymeric  
304 membranes and no one reports separate values of  $CO$  permeability and diffusivity in the examined

305 polymeric membranes, it is worthy to compare transport data obtained with the  $CO_2$ ,  $N_2$  and  $O_2$   
 306 penetrants with literature values to assure the reliability of our experimental approach. Tables V, VI  
 307 and VII present values of gas transport parameters obtained in single gas conditions in experimental  
 308 tests carried out at near-ambient temperature with Matrimid®, PEI and PLA films.

309  
 310  
 311  
 312  
 313

$P_{CO_2}$ (barrer)	$P_{N_2}$ (barrer)	$P_{O_2}$ (barrer)	$D_{CO_2}$ ( $cm^2/s$ )	$D_{N_2}$ ( $cm^2/s$ )	$D_{O_2}$ ( $cm^2/s$ )	Ref.
$8.1 \pm 0.3$	$0.29 \pm 0.02$	$1.8 \pm 0.1$	$(2.2 \pm 0.1) \times 10^{-9}$	$(3.4 \pm 0.2) \times 10^{-9}$	$(1.7 \pm 0.1) \times 10^{-8}$	This work
6.4	0.16	-	-	-	-	21
7.3	0.22	1.46	$3 \times 10^{-9}$	$1 \times 10^{-9}$	$5 \times 10^{-9}$	22
8.9	0.25	1.7	$2.9 \times 10^{-9}$	$2.4 \times 10^{-9}$	$1.3 \times 10^{-8}$	23
9.8	0.31	-	-	-	-	24
7.23	0.21	-	$8.9 \times 10^{-9}$	$4.7 \times 10^{-9}$	-	25

314 Table V: Gas permeability and diffusivity of Matrimid® films measured in single gas permeation tests at  $T =$   
 315  $300 \pm 2$  K and  $p_{feed}$  between 20 and 90 kPa. Experimental conditions of temperature ( $T$ ) and trans-  
 316 membrane pressure ( $\Delta P$ ) for literature data: [21]  $T = 303$  K,  $\Delta P = 2$  to 6 bar; [22]  $T = 298$  K,  $\Delta P = 2$  bar;  
 317 [23]  $T = 293$  K,  $\Delta P = 0.3$  bar; [24]  $T = 298$  K,  $\Delta P = 4$  bar; [25]  $T = 298$  K,  $\Delta P = 10$  bar.

318  
 319  
 320  
 321  
 322

$P_{CO_2}$ (barrer)	$P_{N_2}$ (barrer)	$P_{O_2}$ (barrer)	$D_{CO_2}$ ( $cm^2/s$ )	$D_{N_2}$ ( $cm^2/s$ )	$D_{O_2}$ ( $cm^2/s$ )	Ref.
$1.17 \pm 0.05$	$0.04 \pm 0.01$	$0.32 \pm 0.02$	$(8.5 \pm 0.4) \times 10^{-9}$	$(1.00 \pm 0.04) \times 10^{-8}$	$(3.6 \pm 0.1) \times 10^{-8}$	This work
1.27	-	0.6	-	-	-	26
1.32	0.05	0.4	$3.7 \times 10^{-9}$	-	-	27
1.48	0.05	0.38	-	-	-	28
1.4	0.06	-	-	-	-	29
1.14	-	-	-	-	-	30
1.25	0.05	-	$2.5 \times 10^{-9}$	$2.5 \times 10^{-9}$	-	31
0.2 to 0.3	-	-	-	-	-	32
1.46	0.05	0.4	-	-	-	33

323 Table VI: Gas permeability and diffusivity of PEI films measured in single gas permeation tests at  $T = 295 \pm 2$   
 324 K and  $p_{feed}$  between 20 and 90 kPa. Experimental conditions of temperature ( $T$ ) and trans-membrane  
 325 pressure ( $\Delta P$ ) for literature data: [26]  $T = 298$  K,  $\Delta P = 0.9$  bar ; [27]  $T = 308$  K,  $\Delta P = 10$  bar ; [28]  $T = 308$   
 326 K,  $\Delta P = 3.5$  bar ; [29]  $T = 308$  K,  $\Delta P = 2$  bar ; [30]  $T = 308$  K,  $\Delta P = 3.5$  bar ; [31]  $T = 298$  K,  $\Delta P = 2$  to 5 bar  
 327 ; [32]  $T = 298$  K,  $\Delta P = 2$  to 6 bar; [33]  $T = 308$  K,  $\Delta P = 10$  bar.

328  
 329  
 330  
 331  
 332



333

$P_{CO_2}$ (barrer)	$P_{N_2}$ (barrer)	$P_{O_2}$ (barrer)	$D_{CO_2}$ (cm <sup>2</sup> /s)	$D_{N_2}$ (cm <sup>2</sup> /s)	$D_{O_2}$ (cm <sup>2</sup> /s)	Ref.
$1.12 \pm 0.05$	$0.05 \pm 0.02$	$0.29 \pm 0.02$	$(4.0 \pm 0.2) \times 10^{-9}$	$(7.1 \pm 0.4) \times 10^{-9}$	$(4.3 \pm 0.2) \times 10^{-8}$	This work
1.12	0.04	-	$3.76 \times 10^{-9}$	$7.0 \times 10^{-9}$	-	19
1.1	0.05	0.26	$4.4 \times 10^{-9}$	$2.4 \times 10^{-8}$	$5.7 \times 10^{-8}$	34
1.2	0.05	-	$4.8 \times 10^{-9}$	$2.4 \times 10^{-8}$	-	35
1.71	-	0.13	-	-	-	36

334 Table VII: Gas permeability and diffusivity of PLA films measured in single gas permeation tests at  $T = 298 \pm$   
 335  $2$  K and  $p_{feed}$  values between 20 and 90 kPa. Experimental conditions of temperature ( $T$ ) and trans-  
 336 membrane pressure ( $\Delta P$ ) for literature data: [19]  $T = 300$  K,  $\Delta P = 0.4$  bar; [34]  $T = 303$  K,  $\Delta P =$  not  
 337 reported; [35]  $T = 308$  K,  $\Delta P = 0.5$  to 1 bar; [36]  $T = 298$  K,  $\Delta P = 1$  bar.

338

339

340

341

342

343

344

345

346

347

348

349

350

351

352

353

354

355

356

357

358

359

360

361

362

Looking at data in these Tables we can observe good agreement between our experimental data and literature data. Note also that our ideal  $CO_2/N_2$  selectivity value of  $28 \pm 1$  for Matrimid<sup>®</sup> is coincident with the value of 30 reported in the review of Castro-Munoz *et al.* on Matrimid<sup>®</sup> [37]. Our ideal  $CO_2/N_2$  selectivity value of  $28 \pm 1$  for PEI well compares with literature PEI values ranging from 25 [29] to 30 [33]. Same consideration holds for our ideal  $P_{CO_2}/P_{N_2}$  selectivity values of  $24 \pm 1$  for PLA which well agrees with the value of 22 reported by Bao *et al.* [34] and with the value of 24 reported by Kamatsuka *et al.* [35].

The comparison of activation energy values in Table III and IV with literature data also evidences good compatibility. Activation energy values for permeation in Matrimid<sup>®</sup> range, in fact, from 5.9 to 9.0 kJ/mol for  $CO_2$  and from 13.6 to 20.2 kJ/mol for  $N_2$  [23,38]; no data was found for the activation energy for diffusion. Good compatibility also exists for PLA data: Bao *et al.* obtained activation energy value for permeation of 18.5 and 34.6 kJ/mol for  $CO_2$  and  $N_2$ , respectively [34] while Auras found a value of 15.7 kJ/mol for  $CO_2$  [36]. For  $E_D$  in PLA we only found the value of  $37 \pm 1$  kJ/mol reported by Bao *et al.* for  $CO_2$  [34]. Concerning PEI, we observe that our activation energy values result lower than those indicated by Vega *et al.* which reported an activation energy value of  $32.8 \pm 1.8$  kJ/mol for  $CO_2$  permeation and of  $36.0 \pm 0.3$  kJ/mol for  $CO_2$  diffusion; the authors reported same values, inside the experimental indetermination, for the respective  $N_2$  activation energies [31].

To discuss the  $CO_2/CO$  selective performances of the examined membrane samples, in Table V we report the numerical values of the  $P_\alpha$  and  $D_\alpha$  parameters pertinent to the  $CO_2$  and  $CO$  penetrants, as obtained at near-ambient temperature in permeation tests carried out in single and

363 mixed gas conditions. Corresponding values for  $O_2$  and  $N_2$  are reported in the Supplementary  
 364 Information section, see Tables SI1-SI3.

365

366

		Single Gas	M224	M225
Matrimid® $T = 300 \pm 2$ K	$P_{CO_2}$ (Barrer)	$8.1 \pm 0.3$	$7.9 \pm 0.3$	$8.0 \pm 0.3$
	$D_{CO_2}$ (cm <sup>2</sup> /s)	$(2.2 \pm 0.1) \times 10^{-9}$	$(2.3 \pm 0.1) \times 10^{-9}$	$(2.1 \pm 0.1) \times 10^{-9}$
	$P_{CO}$ (Barrer)	$0.50 \pm 0.03$	$0.54 \pm 0.03$	$0.49 \pm 0.03$
	$D_{CO}$ (cm <sup>2</sup> /s)	$(3.9 \pm 0.2) \times 10^{-9}$	$(3.7 \pm 0.2) \times 10^{-9}$	$(3.8 \pm 0.2) \times 10^{-9}$
PEI $T = 295 \pm 2$ K	$P_{CO_2}$ (Barrer)	$1.17 \pm 0.05$	$1.15 \pm 0.05$	$1.17 \pm 0.05$
	$D_{CO_2}$ (cm <sup>2</sup> /s)	$(8.5 \pm 0.4) \times 10^{-9}$	$(8.0 \pm 0.4) \times 10^{-9}$	$(8.1 \pm 0.4) \times 10^{-9}$
	$P_{CO}$ (Barrer)	$0.07 \pm 0.01$	$0.09 \pm 0.01$	$0.07 \pm 0.01$
	$D_{CO}$ (cm <sup>2</sup> /s)	$(1.08 \pm 0.04) \times 10^{-8}$	$(1.05 \pm 0.05) \times 10^{-8}$	$(1.03 \pm 0.04) \times 10^{-8}$
PLA $T = 298 \pm 2$ K	$P_{CO_2}$ (Barrer)	$1.12 \pm 0.05$	$1.10 \pm 0.05$	$1.10 \pm 0.05$
	$D_{CO_2}$ (cm <sup>2</sup> /s)	$(4.0 \pm 0.2) \times 10^{-9}$	$(3.8 \pm 0.2) \times 10^{-9}$	$(3.8 \pm 0.2) \times 10^{-9}$
	$P_{CO}$ (Barrer)	$0.07 \pm 0.01$	$0.09 \pm 0.01$	$0.08 \pm 0.02$
	$D_{CO}$ (cm <sup>2</sup> /s)	$(9.2 \pm 0.4) \times 10^{-9}$	$(1.00 \pm 0.04) \times 10^{-8}$	$(9.7 \pm 0.6) \times 10^{-8}$

367 Table VIII:  $CO_2$  and  $CO$  transport parameters measured in single gas tests and with the M224 and M225 gas  
 368 mixtures. Permeation tests were carried out with  $p_{feed}$  values between 20 and 90 kPa.  
 369

370 The Matrimid® membrane sample exhibits at near-ambient temperature a single gas  
 371  $P_{CO}$  value of  $0.50 \pm 0.03$  Barrer which is larger than corresponding value for PEI,  $0.07 \pm 0.01$  Barrer,  
 372 and for PLA,  $0.07 \pm 0.01$  Barrer. The ideal  $CO_2/CO$  selectivity values of the examined membrane  
 373 films are equivalent inside their experimental uncertainty: at near-ambient temperature, in fact, the  
 374 ideal  $CO_2/CO$  selectivity value is  $16 \pm 1$  for Matrimid®,  $17 \pm 2$  for PEI and  $16 \pm 2$  for PLA. These  
 375 values are lower than the corresponding ideal  $CO_2/N_2$  selectivity for each membrane sample.

376 As the temperature increases, the ideal  $CO_2/CO$  selectivity of the examined membrane  
 377 samples decreases (see solid symbols in the upper panels of figs. 9-11) reaching the value of  $9.6 \pm$   
 378  $0.4$  for Matrimid® at  $60^\circ\text{C}$ , of  $10 \pm 1$  for PEI at  $69^\circ\text{C}$  and of  $9 \pm 1$  for PLA at  $65^\circ\text{C}$ . Solid symbols in the  
 379 lower panel of figs. 10-12 report the  $D_{CO_2}/D_{CO}$  ratio for the examined membrane samples, as a  
 380 function of temperature. It can be observed that, in the examined temperature interval, the  $CO_2$   
 381 diffusivity is lower than that of  $CO$ : the  $D_{CO_2}/D_{CO}$  ratio is, in fact,  $\sim 0.6$  in Matrimid®,  $\sim 0.7$  in PEI  
 382 and  $\sim 0.4$  in PLA. We can thus conclude that the  $CO_2/CO$  selective properties of all the examined  
 383 membrane samples have mainly a solution-selective character.

384 Indeed, the larger  $CO_2$  solubility in all examined polymer films is clearly favored by the larger  
 385 condensability of the  $CO_2$  specie ( $T_C = 133$  K for  $CO$  and  $304$  K for  $CO_2$ ) [20]: it is worth mentioning,

386 though, that a further positive contribution could arise from weak attractive interactions between  
387 the quadrupolar  $CO_2$  molecule with the aromatic/polar backbones of the polymeric membranes.

388 Looking at Tables III and IV, we observe that sorption in the examined polymeric films has an  
389 exothermic character for both gases. The sorption enthalpy for  $CO$  solution  $\Delta H_S = E_p - E_D$  is  
390 negative and exhibits values of  $-8 \pm 2$  kJ/mol for Matrimid<sup>®</sup>,  $-13 \pm 1$  kJ/mol for PEI and  $-11 \pm 2$   
391 kJ/mol for PLA: all values lie close to the  $CO$  heat of condensation that is  $-6$  kJ/mol [15]. The  $\Delta H_S$   
392 values for  $CO_2$  are in absolute value larger, specifically  $-25 \pm 1$  kJ/mol for Matrimid<sup>®</sup>,  $-19 \pm 1$   
393 kJ/mol for PEI and  $-17 \pm 1$  kJ/mol for PLA, indicating a larger exothermic effect associated with the  
394 sorption of such molecule. As a consequence, being the diffusion activation energy similar for the  
395 two penetrants, and the  $D_{CO_2}/D_{CO}$  ratio essentially constant with temperature, the permeability  
396 increases with temperature more significantly for  $CO$  than for  $CO_2$ , resulting in the decrease of the  
397  $CO_2/CO$  selectivity with temperature.

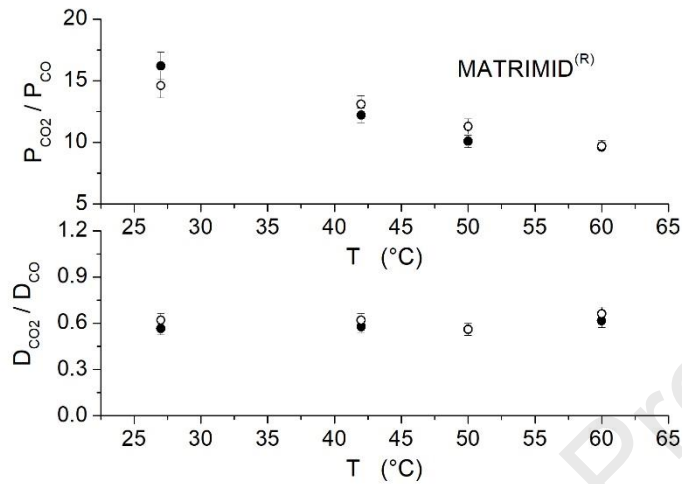
398

399 Looking at Table V we observe that exposing the membrane samples to the ternary,  $CO_2$ -  
400 rich M224 gas mixture at near-ambient temperature, the  $P_{CO_2}$  and  $D_{CO_2}$  values are equal, to within  
401 the experimental accuracy, to values obtained in single gas tests. With the PEI and PLA membrane  
402 we can observe an apparent slight increase of the  $P_{CO}$  value: it's anyway necessary to remark that  
403 this increase is of the same order as the experimental uncertainty. The near-ambient temperature  
404  $CO_2/CO$  selectivity for the Matrimid<sup>®</sup> membrane exposed the  $CO_2$ - rich ternary M224 gas mixture  
405 is similar to the ideal one obtained from pure gas data,  $15 \pm 1$  while it appears slightly decreased  
406 with the PEI membrane,  $13 \pm 2$ , and with the PLA membrane,  $12 \pm 2$ . The  $P$  and  $D$  parameters  
407 pertinent to  $O_2$  obtained with the M224 gas mixture exhibit values equal to those measured in  
408 single gas tests. As in single gas tests, by increasing temperature the  $CO_2/CO$  selectivity of the  
409 examined membrane samples decreases (see open symbols in the upper panel of figs. 9-11) as  
410 discussed above and due to the larger exothermic character of  $CO_2$  sorption. In the examined  
411 temperature interval, membrane samples exhibit  $CO_2/CO$  selectivity values similar to the ideal ones  
412 (see figs. 10 and 11).

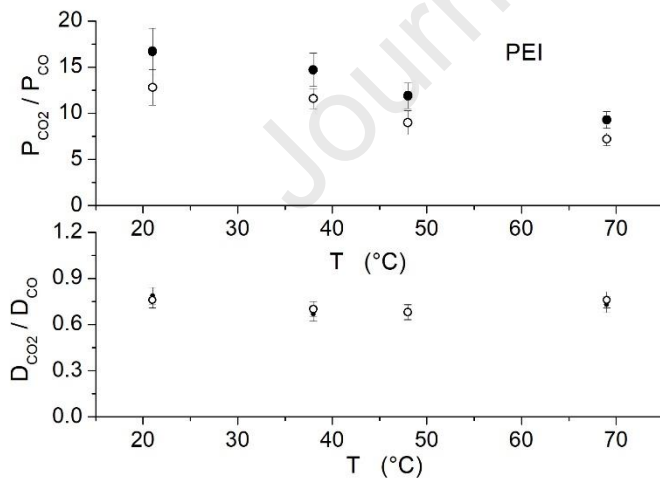
413 Open symbols in the lower panel of figs. 9-11 report the  $D_{CO_2}/D_{CO}$  ratio for the examined  
414 membrane samples, as a function of temperature. Comparing permeability and diffusivity data  
415 obtained in with the  $CO_2$ - rich M224 gas mixture we can conclude that in mixed gas tests the  
416  $CO_2/CO$  separation is determined by the different solution properties of the permeants in the  
417 matrix, similarly to what happens in single gas processes, in the pressure range inspected. It must

418 be reminded that the pressure considered in the tests was sub-atmospheric to reproduce the  
 419 conditions encountered in NTP conversion processes.

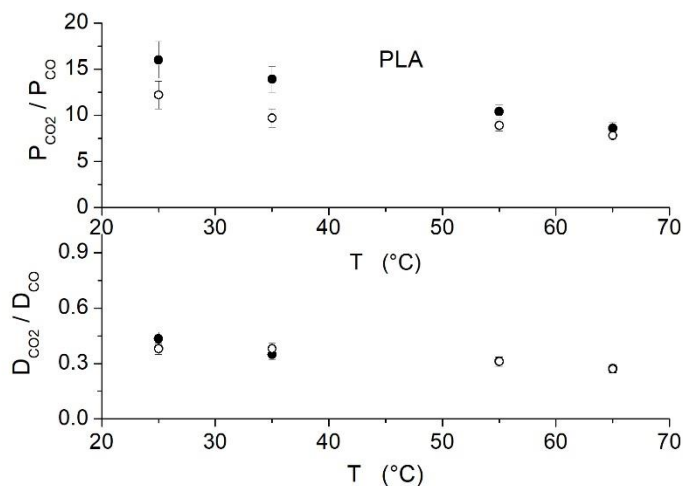
420 We also observe that the  $D_{CO_2}/D_{CO}$  ratio is equal, inside the experimental indetermination,  
 421 to that obtained in single gas tests, evidence that the observed decrease of the  $CO_2/CO$  selectivity  
 422 in multicomponent conditions is caused by the increase of the  $CO$  solubility in the membrane layers  
 423 when exposed to the  $CO_2$ - rich M224 gas mixture.



424  
 425 Fig. 9: Matrimid® membrane. Upper panel:  $CO_2/CO$  selectivity as a function of temperature. Lower panel:  
 426 diffusivity ratio  $D_{CO_2}/D_{CO}$  as a function of temperature. Solid symbols: single gas tests. Open symbols: M224.



427  
 428 Fig. 10: PEI membrane. Upper panel:  $CO_2/CO$  selectivity as a function of temperature. Lower panel:  
 429 diffusivity ratio  $D_{CO_2}/D_{CO}$  as a function of temperature. Solid symbols: single gas test. Open symbols: M224.



430

431 Fig. 11: PLA membrane. Upper panel:  $CO_2/CO$  selectivity as a function of temperature. Lower panel:  
 432 diffusivity ratio  $D_{CO_2}/D_{CO}$  as a function of temperature. Solid symbols: single gas tests. Open symbols: M224.

433

434

435 Looking at Table VIII we observe that the near-ambient temperature  $P_{CO_2}$  and  $D_{CO_2}$  values  
 436 obtained in permeation tests using the quaternary  $CO_2$ -lean M225 gas mixture are equal, to within  
 437 the experimental uncertainty, to the values obtained in single gas tests in all polymers. We also  
 438 observe that the  $P_{CO}$  value results equal, inside its experimental uncertainty, to the value measured  
 439 in single gas tests and the same occurs with the  $D_{CO}$  value. This behavior was observed in the  
 440 examined temperature range, see Tables SI1-SI3, indicating that the  $CO_2/CO$  selectivity of the  
 441 examined membrane samples exposed to the quaternary mixture is comparable to the ideal one,  
 442 maybe due to the lower content of  $CO_2$  in this mixture. The  $CO_2/CO$  selectivity decreases, indeed,  
 443 from  $16 \pm 1$  at near-ambient temperature to  $10 \pm 1$  at  $60^\circ C$  with Matrimid®, from  $17 \pm 2$  at near-  
 444 ambient temperature to  $10 \pm 1$  for PEI and from  $15 \pm 2$  at near-ambient temperature to  $9 \pm 1$  at  
 445  $65^\circ C$  with PLA.

446

447 Comparing  $CO_2$  data obtained in single and mixed gas tests we observe that the presence of  
 448  $CO$  in the feed gas mixture does not alter the  $CO_2$  transport rates, suggesting that possible  
 449 interactions of the polar  $CO$  molecule with segments of the polymer chains as well as competitive  
 450 sorption in the polymer layers between  $CO$  and  $CO_2$  do not play a role in this transport process.

451 Our experimental results indicate that the  $CO$  transport rates using the M224 gas mixture  
 452 are slightly larger than those obtained in single gas test, while using the M225 gas mixture no  
 453 difference is observed. The  $CO_2$  content of the M225 mixture is half that in the M224 one,

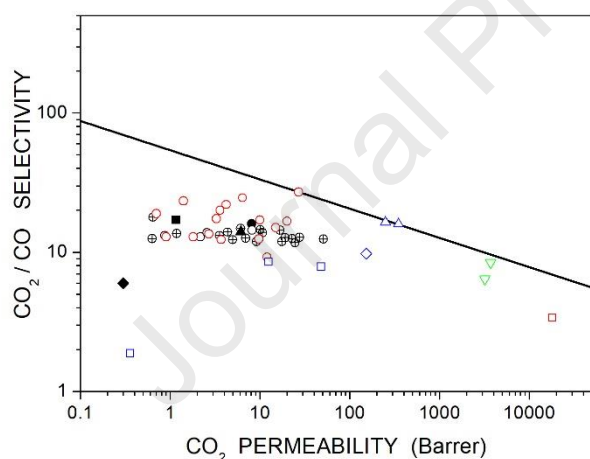
454 suggesting that the increase of the  $CO$  transport rates using the M224 gas mixture is connected to  
455 the higher fraction of  $CO_2$  molecules dissolved in the polymer. However, the  $P_{CO}$  increase cannot  
456 be attributed to  $CO_2$  induced plasticization effects: plasticization occurs, in fact, exposing the  
457 polymer films to much larger  $CO_2$  pressures than those used for the present experimental tests (at  
458 least 8-10 bar with Matrimid<sup>®</sup>, for example [39]). Moreover, experimental results do not show any  
459 increase of the  $CO_2$  transport rates with the gas mixtures, which should be indicative of  
460 plasticization. Possible explanations are minor variations of the free volume size distribution upon  
461  $CO_2$  dissolution favoring the  $CO$  molecular sorption or weak interactions between the quadrupolar  
462  $CO_2$  and polar  $CO$  molecules.

463 Note that the scientific literature reports only moderate changes between gas permeability  
464 values obtained in single gas and in mixed gas tests sometimes observed in studies dedicated to the  
465 separation of  $CO_2/CH_4$  binary gas mixtures [40,41]. Furthermore, multicomponent effects are more  
466 visible at higher pressures, while the experimental range examined here is sub-atmospheric, as  
467 discussed above.

468  
469 It is worthy to compare the measured  $CO_2/CO$  selective performances of the studied  
470 membrane samples with literature data. Dense Matrimid<sup>®</sup> films have been studied by David *et al.*:  
471 the authors measured at 303 K in single gas tests with 2 to 6 atm feed pressure a  $P_{CO_2}$  value of 6.4  
472 Barrer and  $CO_2/CO$  ideal selectivity  $\sim 14$  [21]. Scholes *et al.* studied the separation properties of  
473 Matrimid<sup>®</sup> membranes exposed to gas mixtures (16.2 %  $CO_2$ , 9.8 %  $H_2$ , 63.2 %  $N_2$ , 6.7 %  $CO$ , 2.8 %  
474  $CH_4$ ) and evaluated at 308 K a  $P_{CO_2}$  value of 7.8 Barrer with  $CO_2/CO$  ideal selectivity of 3.3 [42].  
475 Hamidavi *et al.* studied neat polyetherimide (PEI) films and measured at near-ambient temperature  
476 a  $P_{CO_2}$  value of 0.2 to 0.3 Barrer with ideal selectivity of 6: the authors evaluated a  $CO$  activation  
477 energy value for permeation of 78.72 kJ/mol in the 300 to 328 K temperature interval [30]. These  
478 data are presented in fig. 12 together with selectivity data obtained in the present study: for sake  
479 of comparison here we also present  $CO_2/CO$  selectivity values vs.  $P_{CO_2}$  values obtained from a paper  
480 by Michaels *et al.* dedicated to a study of the flow of gases through polyethylene (PE) films with  
481 different crystalline content [43]. This figure also shows literature data on the  $CO_2/CO$  separation  
482 properties of amorphous polymeric membranes prepared using different kind of fluorinated and  
483 non-fluorinated polyimides measured in single gas tests at 323 K with 10 atm feed pressure [44,45]  
484 and at 298 K [46], data obtained by Cao *et al.* in a study on the permeation of gases through  
485 polyurethane-polycarbonate membranes at 308 K in single gas tests [47], data pertinent to rubbery

486 poly(dimethylsiloxane) (PDMS), to a glassy PTMSP poly(1-trimethylsilyl-1-propyne) (PTMSP)  
 487 membrane exposed at 308 K to a simulated syngas (1.5 %  $H_2S$ , 10.5 %  $CO_2$ , 46%  $CO$  and 42 %  $H_2$ )  
 488 [48] and to rubbery polyether-polyamine (Pebax) membranes at 308 K with 10 atm feed pressure in  
 489 single gas conditions [49]. More detailed information can be found in the Supplementary  
 490 Information section, see Table SI4.

491 Fig. 12 contains also the upper bond correlation among selectivity and permeability for the  
 492 separation of the gas couple  $CO_2/CO$ , in the trade-off correlation (Robeson's plot), proposed in this  
 493 work for the first time. It is noteworthy that such upper bound line in the log-log plot was  
 494 determined in a purely empirical fashion, similarly to the original reference and was found to be  
 495  $\alpha = 54/P^{0.21}$  [50,51]. It appears from the plot that Matrimid® does not lie exactly on the upper  
 496 bound but has intermediate values of permeability and selectivity that could make it a good  
 497 candidate for the removal of  $CO_2$  from  $CO$ - containing streams, such as those coming from NTP  
 498 conversion



499

500 Fig. 12:  $CO_2/CO$  selectivity vs.  $CO_2$  permeability. Continuous line refers to the proposed upper-bound  
 501 correlation similar to the Robeson's plot curve [50,51]. Solid black circle and solid black squares refer to the  
 502 Matrimid® and PEI films tested in the present study. Open black triangle: Matrimid® film [21]. Open black  
 503 diamond: Ultem® film [32]. Crossed circles: polyimide films [44,45]. Open red circles: polyurethane-  
 504 polycarbonate films [47]. Open blue squares: polyethylene films [42]. Open blue diamond: natural rubber  
 505 [42]. Open blue triangles: polyether-polyamine films [49]. Open red square: poly(1-trimethylsilyl-propyne)  
 506 film [48]. Open green triangle: polydimethyl siloxane films [48].

507

508

509

## Conclusions

510

511

512

The pure and mixed gas permeation of  $CO_2$ - rich gas mixtures containing  $CO$ ,  $O_2$  and  $N_2$  have been investigated for Matrimid®, PEI and PLA membrane films with the aim of exploring such materials in the purification of mixtures coming from the process of  $CO_2$  reforming by non-thermal

513 plasma. Data were obtained with a novel mass spectrometric apparatus which allows to monitor  
514 accurately the permeate mixture composition as a function of time, and thus obtained  
515 multicomponent diffusivity and permeability values. Single-gas tests indicate that the examined  
516 membrane samples present near-ambient temperature values  $\sim 17$  for the ideal  $CO_2/CO$  selectivity  
517 offering the Matrimid<sup>®</sup> membrane the highest  $CO$  permeability value,  $0.50 \pm 0.03$  Barrer. Increasing  
518 temperature, the ideal  $CO_2/CO$  selectivity of all samples decreases reaching Matrimid<sup>®</sup> a selectivity  
519 value of  $\sim 10$  at  $60^\circ\text{C}$ . In the studied membrane samples, the  $CO_2/CO$  selectivity has a solution-  
520 selective character. Indeed,  $CO_2$  is always the more permeable component in the mixture despite  
521 having a smaller diffusivity than  $CO$ , thanks to its high solubility in the polymers, which is largely due  
522 to its higher condensability. The  $CO_2/CO$  selectivity decreases with temperature for all polymers,  
523 which is consistent with previous data on other polymers and with the fact that the  $CO_2$  sorption  
524 has a larger exothermic effect than that of  $CO$ . The  $CO_2$  permeability and diffusivity values do not  
525 show significant variations compared to single gas tests using  $CO_2$ - rich gases as feed mixture and  
526 only a limited increase of the  $CO$  transport rate is observed in the presence of high amounts of  $CO_2$   
527 in the mixture.

528 A tentative Robeson's upper bound has been drawn for the  $CO_2/CO$  mixture for which there  
529 is lack of data in the literature, and very poor analysis of the obtained results. By looking at this plot,  
530 it can be concluded that Matrimid<sup>®</sup>, lying approximately at the middle of the curve with  
531 intermediate values of permeability and selectivity could be a good candidate as membrane for the  
532 removal of  $CO_2$  from mixtures containing  $CO$ , such as those coming from plasma reformed mixtures  
533 and syngas.

534

535



536 **References**

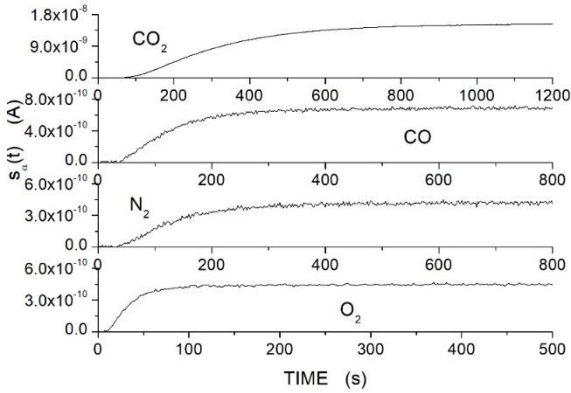
- 537 [1] B. Ashford, Y. Wang, L. Wang and X. Tu, in *Plasma Catalysis, Fundamentals and Applications*, X. Tu, J. C.  
 538 Whitehead and T. Nozaki (Springer Nature, Switzerland, 2019).
- 539 [2] R. Snoeckx and A. Bogaerts, *Plasma technology – a novel solution for CO<sub>2</sub> conversion?* Chem. Soc. Rev. **46**  
 540 (2017) 5805–5863.
- 541 [3] S. D. Kenarsari, D. Yang, G. Jiang, S. Zhang, J. Wang, A. G. Russel, Q. Wei and M. Fan, *Review of recent*  
 542 *advances in carbon dioxide separation and capture*, RCS Adv. **3** (2013) 22739–22773.
- 543 [4] A. Brunetti, P. Bernardo, G. Barbieri, *Membrane Engineering: Progress and Potentialities in gas Separation*,  
 544 in: Y. Yampolskii and B. Freeman (Eds.), *Membrane Gas Separation*, John Wiley and Sons, Chichester, 2010,  
 545 pp.281.
- 546 [5] C. Higman and M. van der Burgt, *Gasification* (Elsevier, London, 2008).
- 547 [6] M. Monteleone, A. Fuoco, E. Esposito, I. Rose, J. Chen, B. Comesana-Gandara, C. G. Bezzu, M. Carta, N. B.  
 548 Mckeown, M. G. Shaligyn, V. V. Teplyakov and J. C. Jansen, *Advanced methods for analysis of mixed gas*  
 549 *diffusion in polymeric membranes*, J. Membrane Sci. **648** (2022) 120356.
- 550 [7] H. Ohya, V. V. Kudruvtsev and S. I. Semenova, *Polyimides Membranes* (Gordon and Breach Publishers:  
 551 Amsterdam, The Netherlands 1996).
- 552 [8] M. J. Troughton, *Handbook of plastic joining: a practical guide*, Elsevier Inc., 2008.
- 553 [9] A. Farah, D. G. Anderson and R. Langer, *Physical and mechanical properties of PLA and their functions in*  
 554 *widespread applications – a comprehensive review*, Adv. Drug Delivery Rev. **107** (2016) 367–392.
- 555 [10] X. Y. Chen, S. Kaliaguine and D. Rodrigue, *A Comparison between Several Commercial Polymer Hollow*  
 556 *Fiber Membranes for Gas Separation*, J. Mem. Sep. Technol. **6** (2017) 1–15.
- 557 [11] E. Esposito, L. Dellamuzia, U. Moretti, A. Fuoco, L. Giorno and J. C. Jansen, *Simultaneous production of*  
 558 *biomethane and food grade CO<sub>2</sub> from biogas: an industrial case study*, Energy Environ. Sci. **12** (2019) 281–  
 559 289.
- 560 [12] S. R. Reijerkerk, K. Nijmeijer, C. P. Ribeiro, B. D. Freeman and M. Wessling *On the effects of plasticization*  
 561 *in CO<sub>2</sub>/light gas separation using polymeric solubility selective membranes* J. Membrane Sci. **2011**, 367, 33–  
 562 44 ; R. Swaidan, B. Ghanem, M. Al-Saeedi, E. Litwiller, I. Pinnau, *Role of intrachain rigidity in the plasticization*  
 563 *of intrinsically microporous triptycene-based polyimide membranes in mixed-gas CO<sub>2</sub>/CH<sub>4</sub> separations*,  
 564 *Macromolecules* **2014**, 47, 7453–7462 ; G. Genduso, B. S. Ghanem and I. Pinnau, *Experimental mixed-gas*  
 565 *permeability, sorption and diffusion of CO<sub>2</sub>-CH<sub>4</sub> mixtures in 6FDA-MPDA polyimide membranes: unveiling the*  
 566 *effect of competitive sorption on permeability selectivity*, Membranes 2019 Jan, 9(1). doi:  
 567 10.3390/membranes9010010.
- 568 [13] L. M. Martini, S. Lovascio, G. Dilecce and P. Tosi, *Time-Resolved CO<sub>2</sub> Dissociation in a Nanosecond Pulsed*  
 569 *Discharge*, Plasma Chem. Plasma Proc. **38** (2018) 707–718.
- 570 [14] L. M. Martini, N. Gatti, G. Dilecce, M. Scotoni, P. Tosi *Rate constants of quenching and vibrational*  
 571 *relaxation in the OH (A<sup>2</sup>Σ<sup>+</sup>, v = 0, 1) manifold with various colliders*, J. Phys. D Appl. Phys. **50** (2017) 114003.
- 572 [15] P. A. Redhead, J. P. Hobson and E. V. Kornelsen, *The Physical Basis of Ultrahigh Vacuum* (AIP, New York,  
 573 1993).
- 574 [16] R. Checchetto, *Accurate monitoring of gas mixture transport kinetics through polymeric membranes*,  
 575 *Sep. Purif. Technol.* **277** (2021) 119477.
- 576 [17] J. G. Wijmans and R. W. Backer, *The solution-diffusion model: a review*, J. Membrane Sci. **107** (1995) 1–  
 577 21.
- 578 [18] Clem E. Powell and Greg G. Qiao, *Polymeric CO<sub>2</sub>/N<sub>2</sub> gas separation membranes for the capture of carbon*  
 579 *dioxide from power plant flue gases*, J. Membrane Sci. **279** (2006) 1–49.
- 580 [19] M. Dickerman, S. Tarter, W. Egger, A. Pegoretti, D. Rigotti, R. S. Brusa and R. Checchetto, *Interface*  
 581 *nanocavities in poly(lactic acid) membranes with dispersed cellulose nanofibrils: their role in the gas barrier*  
 582 *performances*, Polymer **202** (2020) 122729.
- 583 [20] *Transport of Gases and Vapors in Glassy and Rubbery Polymers*, S. Matteucci, Y. Yampolskii, B. D.  
 584 Freeman and I. Pinneau, in *Materials Science of Membranes for Gas and Vapor Separation*, Y. Yampolskii, I.  
 585 Pinneau and B. D. Freeman Eds. (2006 John Wiley & Sons).

- 586 [21] O. C. David, D. Gorri, A. M. Urriaga and I. Ortiz, *Mixed gas separation study for the hydrogen recovery*  
587 *from H<sub>2</sub>/CO/N<sub>2</sub>/CO<sub>2</sub> post combustion mixtures using a Matrimid membrane*, J. Membrane Sci. **378** (2011)  
588 359-368.
- 589 [22] Y. Zhang, K. J. Balkus Jr., I. H. Musselman and J. P. Ferraris, *Mixed-matrix membranes composed of*  
590 *Matrimid and mesoporous ZSM-5 nanoparticles*, J. Membrane Sci. **325** (2008) 28-39.
- 591 [23] S. Shishatskiy, C. Nestor, M. Popa, S. P. Nunes and K. V. Peinemann, *Polyimide asymmetric membranes*  
592 *for hydrogen separation: influence of formation conditions on gas transport properties*, Adv. Eng. Mater. **8**  
593 (2006) 390-397.
- 594 [24] A. Mirzaei, A. H. Navarchian and S. Tangestaninejad, *Mixed matrix membranes on the basis of Matrimid*  
595 *and palladium zeolitic imidazolate framework for hydrogen separations*, Iran. Polym. J. **29** (2020) 479-491.
- 596 [25] A. L. Khan, K. X. Li and Ivo F. J. Vankelecom, *SPEEK/Matrimid blend membranes for CO<sub>2</sub> separation*, J.  
597 Membrane Sci. **380** (2011) 55-62.
- 598 [26] N. M. Larocca and L. A. Pessan *Effect of antiplasticization on the volumetric, gas sorption and transport*  
599 *properties of polyetherimide*, J. Membrane Sci. **218** (2003) 69-92.
- 600 [27] T. A. Barbari, W. J. Koros and D. R. Paul, *Polymeric membranes based on bisphenol-a for gas separation*,  
601 J. Membrane Sci. **42** (1989) 69-86.
- 602 [28] I. Hao, P. Li and T. S. Chun, *PIM-1 as an organic filler to enhance the gas separation performances of*  
603 *Ultem polyetherimide*, J. Membrane Sci. **453** (2014) 614-623.
- 604 [29] Y. Dai, J. R. Johnson, O. Karvan, D. S. Sholl, W. J. Koros, *Ultem®/ZIF-8 mixed hollow fiber matrix*  
605 *membranes for CO<sub>2</sub>/N<sub>2</sub> separations*, J. Membrane Sci. **401-402** (2012) 76-82.
- 606 [30] C. Duan, G. Kang, D. Liu, L. Wang, C. Jiang and Q. Yuan, *Enhanced gas separation properties of metal*  
607 *organic framework/polyetherimide mixed matrix membranes*, J. Appl. Polym. Sci. **131** (2014) 8828-8837.
- 608 [31] J. Vega, A. Andrio, A. A. Lemus, J. A. I. Diaz, L. F. del Castillo, R. Gavara and V. Compan, *Modification of*  
609 *polyetherimide membranes with ZIFs fillers for CO<sub>2</sub> separation*, Sep. Purif. Technol. **212** (2019) 474-482.
- 610 [32] F. Hamidavi, A. Kargari and A. Eliassi, *Sorption and permeation study of polyetherimide/hydrophobic silica*  
611 *nanocomposite membranes for effective syngas (H<sub>2</sub>/CO/CO<sub>2</sub> separation*, Sep. Purif. Technol. **279** (2021)  
612 119774.
- 613 [33] X. Y. Chen, S. Kaliaguine and D. Rodrigue, *A Comparison between Several Commercial Polymer Hollow*  
614 *Fiber Membranes for Gas Separation*, J. Mem. Sep. Technol. **6** (2017) 1-15.
- 615 [34] L. Bao, J. R. Dorgan, D. Knauss, S. hait, N. S. Oliver and I. M. Maruccho, *Gas permeation properties of*  
616 *poly(lactic acid) revisited*, J. Membrane Sci. **285** (2006) 166-172.
- 617 [35] T. Komatsuka, A. Kusakabe and K. Nagai, *Characterization and gas transport properties of poly(lactic*  
618 *acid) blend membranes*, Desalination **234** (2008) 212-220.
- 619 [36] R. A. Auras, B. Harte, S. Selke and R. Hernandez, *Mechanical, physical, and barrier properties of poly(lactic*  
620 *acid) films*, J. Plas. Films Sheet. **19** (2003) 123-135.
- 621 [37] R. Castro-Munoz, V. Martin-Gil, M. Z. Ahmad and V. Fila, *Matrimid 5218 in preparation of membranes*  
622 *for gas separation: current state-of-art*, Chem. Eng. Comm. **205** (2017) 161-196.
- 623 [38] H. Y. Zhao, Y. M. Cao, X. L. Ding, M. Q. Zhou, Q. Yuan, *Effects of cross-linkers with different molecular*  
624 *weights in cross-linked Matrimid 5218 and test temperature on gas transport properties*, J. Membrane Sci.  
625 **323** (2008) 176-184.
- 626 [39] A. Bos, I. M. G. Punt, M. Wessling and H. Strathmann, *CO<sub>2</sub>- induced plasticization phenomena in glassy*  
627 *polymers*, J. Membrane Sci. **155** (1999) 67-78.
- 628 [40] Y. Zhang, K. J. Balkus Jr., I. H. Musselman and J. P. Ferraris, *Mixed-matrix membranes composed of*  
629 *Matrimid and mesoporous ZSM-5 nanoparticles*, J. Membrane Sci. **325** (2008) 28-39.
- 630 [41] S. Shahid and K. Nijmeijer, *Performance and plasticization of polymer-MOF membranes for gas*  
631 *separation at elevated pressures*, J. Membrane Sci. **470** (2014) 166-177.
- 632 [42] C. A. Scholes, G. Q. Chen, W. X. Tao, J. Bacus, C. Anderson, G. W. Stevens and S. E. Kentish, *The effect of*  
633 *minor components on the gas separation performances of membranes for carbon capture*, Energy Procedia **4**  
634 (2011) 681-687.
- 635 [43] A. S. Michaels and H. J. Bixler, *Flow of gases through polyethylene*, J. Polym. Sci. **1** (1961) 413-439.
- 636 [44] K. Tanaka, H. Kita, K. Okamoto, A. Nakamura and Y. Kusuki, *Gas permeability and permselectivity in*  
637 *polyimides based on 3,3', 4,4' -biphenyltetracarboxylic dianhydride*, J. Membrane Sci. **47** (1989) 203-215.

- 638 [45] K. Tanaka, H. Kita, M. Okano and K.Okamoto, *Permeability and permeselectivity of gases in fluorinated*  
639 *and non-fluorinated polyimides*, *Polymer* **33** (1992) 585-592.
- 640 [46] K. Haraya, K. Obata, T. Hakuta and H. Yoshitome, *The permeation of gases through a new type of*  
641 *polyimide membranes*, *Membrane* **11** (1986) 48-52.
- 642 [47] N. Cao, M. Pegoraro, F. Bianchi, L. Di Landro and L. Zanderighi, *Gas transport properties of polycarbonate-*  
643 *polyurethane membranes*, *J. Appl. Polym. Sci.* **48** (1993) 1831-1842.
- 644 [48] T. C. Merkel, R. P. Gupta, B. S. Turk and B. D. Freeman, *Mixed gas permeation of syngas components in*  
645 *poly(dimethylsiloxane) and poly(1-trimethylsilyl-1-popyne) at elevated temperature*, *J. Membrane Sci.* **191**  
646 (2001) 85-94.
- 647 [49] B. Wilks and M. E. Rezac, *Properties of rubbery polymers for the recovery of hydrogen sulfide from*  
648 *gasification gases*, *J. Appl. Polym. Sci.* **85** (2002) 2436-2444.
- 649 [50] L. M. Robeson, *Correlation of separation factors versus permeability for polymeric membranes*, *J.*  
650 *Membrane Sci.* **62** (1991) 165-185.
- 651 [51] L. M. Robeson, *The upper bound revisited*, *J. Membrane Sci.* **320** (2008) 390-400.
- 652
- 653

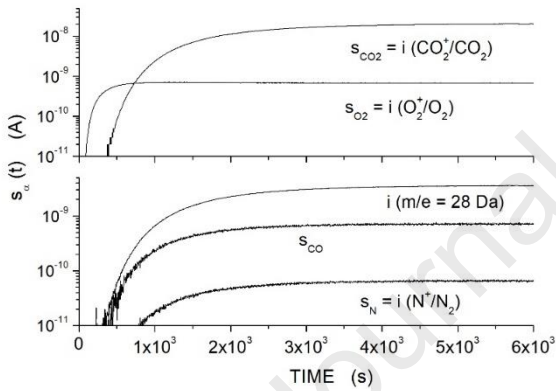
654  
655  
656  
657

SUPPLEMENTARY INFORMATION



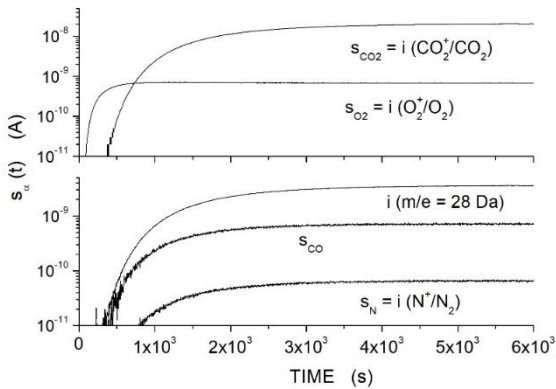
658  
659  
660  
661  
662

Fig. SI1:  $s_{\alpha}(t)$  mass signals obtained at  $T = 298 \pm 2$  K with the PLA film sample exposed to pure  $CO_2$ ,  $CO$  and  $N_2$  gases ( $p_{feed} = 45 \pm 1$  kPa) and to the dry  $N_2/O_2$  air mixture ( $p_{feed} = 72 \pm 1$  kPa).



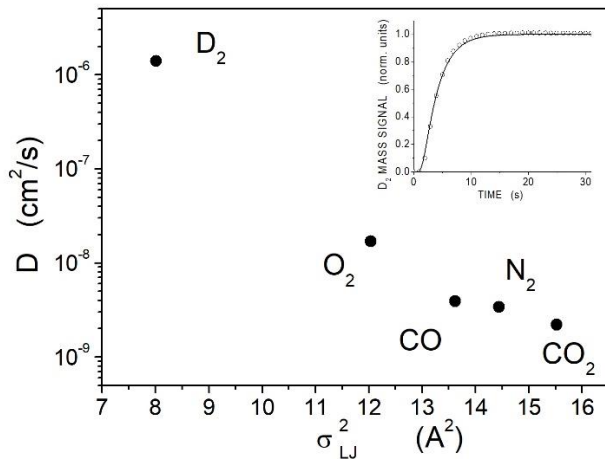
663  
664  
665  
666  
667

Fig. SI2:  $s_{\alpha}(t)$  mass signals obtained at  $T = 295 \pm 2$  K with the PEI film sample exposed to the M224 gas mixture ( $p_{feed} = 45 \pm 1$  kPa).



668  
669  
670  
671  
672

Fig. SI3:  $s_{\alpha}(t)$  mass signals obtained at  $T = 300 \pm 2$  K with the Matrimid® film sample exposed to the M225 gas mixture ( $p_{feed} = 72 \pm 1$  kPa).



673  
674  
675  
676  
677  
678  
679  
680  
681

Fig. SI4: Plot of the diffusivity value of the examined penetrants in Matrimid® obtained at  $T = 300 \pm K$  as a function of the squared Lennard-Jones molecular size ( $\sigma_{LJ}$  values are reported in Table II). The deuterium ( $D_2$ ) diffusivity value is also reported. This value was evaluated fitting by eq. 5 a normalized  $D_2$  permeation curve obtained at  $T = 300 \pm 2 K$  and feed pressure of 40 kPa (see inset).

Matrimid®		300 ± 2 K	315 ± 2 K	323 ± 2 K	333 ± 2 K
$P_{CO_2}$ (Barrer)	SG	8.1 ± 0.3	9.5 ± 0.3	10.1 ± 0.3	11.1 ± 0.3
	M224	7.9 ± 0.3	9.7 ± 0.3	10.0 ± 0.3	11.3 ± 0.3
	M225	8.0 ± 0.3	9.6 ± 0.3	10.0 ± 0.3	11.2 ± 0.3
$P_{CO}$ (Barrer)	SG	0.50 ± 0.03	0.77 ± 0.03	1.00 ± 0.04	1.14 ± 0.04
	M224	0.54 ± 0.03	0.74 ± 0.03	0.81 ± 0.05	1.16 ± 0.04
	M225	0.49 ± 0.03	0.75 ± 0.03	0.95 ± 0.06	1.13 ± 0.06
$D_{CO_2}$ (cm²/s)	SG	$(2.2 \pm 0.1) \times 10^{-9}$	$(4.1 \pm 0.1) \times 10^{-9}$	$(5.2 \pm 0.2) \times 10^{-9}$	$(8.0 \pm 0.3) \times 10^{-9}$
	M224	$(2.3 \pm 0.1) \times 10^{-9}$	$(4.2 \pm 0.1) \times 10^{-9}$	$(5.0 \pm 0.2) \times 10^{-9}$	$(7.5 \pm 0.3) \times 10^{-9}$
	M225	$(2.1 \pm 0.1) \times 10^{-9}$	$(4.1 \pm 0.1) \times 10^{-9}$	$(5.1 \pm 0.2) \times 10^{-9}$	$(7.6 \pm 0.3) \times 10^{-9}$
$D_{CO}$ (cm²/s)	SG	$(3.9 \pm 0.2) \times 10^{-9}$	$(7.1 \pm 0.3) \times 10^{-9}$	$(9.3 \pm 0.3) \times 10^{-9}$	$(1.22 \pm 0.05) \times 10^{-8}$
	M224	$(3.7 \pm 0.2) \times 10^{-9}$	$(6.7 \pm 0.3) \times 10^{-9}$	$(9.0 \pm 0.3) \times 10^{-9}$	$(1.14 \pm 0.05) \times 10^{-8}$
	M225	$(3.8 \pm 0.2) \times 10^{-9}$	$(6.8 \pm 0.3) \times 10^{-9}$	$(9.0 \pm 0.3) \times 10^{-9}$	$(1.16 \pm 0.05) \times 10^{-8}$
$P_{O_2}$ (Barrer)	SG	1.8 ± 0.1	2.6 ± 0.1	3.1 ± 0.1	3.4 ± 0.1
	M224	1.8 ± 0.1	2.6 ± 0.1	3.0 ± 0.1	3.4 ± 0.2
	M225	1.7 ± 0.1	2.7 ± 0.1	3.0 ± 0.1	3.3 ± 0.1
$D_{O_2}$ (cm²/s)	SG	$(1.7 \pm 0.1) \times 10^{-8}$	$(2.7 \pm 0.1) \times 10^{-8}$	$(3.2 \pm 0.1) \times 10^{-8}$	$(4.5 \pm 0.1) \times 10^{-8}$
	M224	$(1.7 \pm 0.1) \times 10^{-8}$	$(2.7 \pm 0.1) \times 10^{-8}$	$(3.1 \pm 0.1) \times 10^{-8}$	$(3.9 \pm 0.2) \times 10^{-8}$
	M225	$(1.7 \pm 0.1) \times 10^{-8}$	$(2.8 \pm 0.1) \times 10^{-8}$	$(3.2 \pm 0.1) \times 10^{-8}$	$(4.2 \pm 0.2) \times 10^{-8}$
$P_{N_2}$ (Barrer)	SG	0.29 ± 0.02	0.44 ± 0.02	0.50 ± 0.02	0.65 ± 0.02
	M225	0.27 ± 0.03	0.42 ± 0.03	0.51 ± 0.03	0.64 ± 0.03
$D_{N_2}$ (cm²/s)	SG	$(3.4 \pm 0.2) \times 10^{-9}$	$(5.9 \pm 0.2) \times 10^{-9}$	$(8.0 \pm 0.2) \times 10^{-9}$	$(1.10 \pm 0.03) \times 10^{-9}$
	M225	$(3.4 \pm 0.3) \times 10^{-9}$	$(6.0 \pm 0.3) \times 10^{-9}$	$(8.3 \pm 0.3) \times 10^{-9}$	$(1.10 \pm 0.05) \times 10^{-9}$

682 Table SI1: Permeability and diffusivity numerical values of  $CO_2$ ,  $O_2$ ,  $N_2$  and  $CO$  in the Matrimid® membrane sample  
683 ( $p_{feed}$  between 20 and 90 kPa).  
684  
685  
686  
687  
688  
689

690  
691

PEI		295 ± 2 K	311 ± 2 K	321 ± 2 K	342 ± 2 K
$P_{CO_2}$ (Barrer)	SG	1.17 ± 0.05	1.18 ± 0.05	1.19 ± 0.05	1.24 ± 0.05
	M224	1.15 ± 0.05	1.16 ± 0.05	1.17 ± 0.05	1.22 ± 0.05
	M225	1.17 ± 0.05	1.16 ± 0.05	1.18 ± 0.05	1.24 ± 0.05
$P_{CO}$ (Barrer)	SG	0.07 ± 0.01	0.08 ± 0.01	0.10 ± 0.01	0.12 ± 0.01
	M224	0.09 ± 0.01	0.10 ± 0.01	0.13 ± 0.01	0.17 ± 0.01
	M225	0.07 ± 0.01	0.09 ± 0.01	0.11 ± 0.01	0.12 ± 0.01
$D_{CO_2}$ (cm <sup>2</sup> /s)	SG	$(8.5 \pm 0.4) \times 10^{-9}$	$(1.20 \pm 0.05) \times 10^{-8}$	$(1.7 \pm 0.1) \times 10^{-8}$	$(2.7 \pm 0.1) \times 10^{-8}$
	M224	$(8.0 \pm 0.4) \times 10^{-9}$	$(1.20 \pm 0.05) \times 10^{-8}$	$(1.5 \pm 0.1) \times 10^{-8}$	$(2.8 \pm 0.1) \times 10^{-8}$
	M225	$(8.1 \pm 0.4) \times 10^{-9}$	$(1.20 \pm 0.05) \times 10^{-8}$	$(1.7 \pm 0.1) \times 10^{-8}$	$(2.8 \pm 0.1) \times 10^{-8}$
$D_{CO}$ (cm <sup>2</sup> /s)	SG	$(1.08 \pm 0.04) \times 10^{-8}$	$(1.95 \pm 0.07) \times 10^{-8}$	$(2.5 \pm 0.1) \times 10^{-8}$	$(3.7 \pm 0.1) \times 10^{-8}$
	M224	$(1.05 \pm 0.04) \times 10^{-8}$	$(1.72 \pm 0.07) \times 10^{-8}$	$(2.2 \pm 0.1) \times 10^{-8}$	$(3.7 \pm 0.1) \times 10^{-8}$
	M225	$(1.03 \pm 0.04) \times 10^{-8}$	$(1.81 \pm 0.07) \times 10^{-8}$	$(2.4 \pm 0.1) \times 10^{-8}$	$(3.6 \pm 0.1) \times 10^{-8}$
$P_{O_2}$ (Barrer)	SG	0.32 ± 0.02	0.35 ± 0.02	0.38 ± 0.02	0.50 ± 0.02
	M224	0.30 ± 0.02	0.34 ± 0.02	0.37 ± 0.02	0.49 ± 0.02
	M225	0.32 ± 0.02	0.35 ± 0.02	0.37 ± 0.02	0.50 ± 0.02
$D_{O_2}$ (cm <sup>2</sup> /s)	SG	$(3.6 \pm 0.1) \times 10^{-8}$	$(5.0 \pm 0.1) \times 10^{-8}$	$(6.0 \pm 0.1) \times 10^{-8}$	$(9.5 \pm 0.1) \times 10^{-8}$
	M224	$(3.5 \pm 0.1) \times 10^{-8}$	$(5.1 \pm 0.1) \times 10^{-8}$	$(6.0 \pm 0.1) \times 10^{-8}$	$(9.3 \pm 0.1) \times 10^{-8}$
	M225	$(3.4 \pm 0.1) \times 10^{-8}$	$(5.2 \pm 0.1) \times 10^{-8}$	$(6.1 \pm 0.1) \times 10^{-8}$	$(9.5 \pm 0.1) \times 10^{-8}$
$P_{N_2}$ (Barrer)	SG	0.04 ± 0.01	0.04 ± 0.01	0.05 ± 0.01	0.07 ± 0.01
	M225	0.05 ± 0.02	0.04 ± 0.02	0.05 ± 0.01	0.07 ± 0.01
$D_{N_2}$ (cm <sup>2</sup> /s)	SG	$(1.01 \pm 0.03) \times 10^{-8}$	$(2.00 \pm 0.03) \times 10^{-8}$	$(2.24 \pm 0.03) \times 10^{-8}$	$(3.51 \pm 0.03) \times 10^{-8}$
	M225	$(1.1 \pm 0.1) \times 10^{-8}$	$(2.0 \pm 0.1) \times 10^{-8}$	$(2.3 \pm 0.1) \times 10^{-8}$	$(3.4 \pm 0.1) \times 10^{-8}$

692 Table S12: Permeability and diffusivity numerical values of  $CO_2$ ,  $O_2$ ,  $N_2$  and  $CO$  in the PEI membrane sample ( $p_{feed}$   
693 between 20 and 90 kPa).  
694  
695

PLA		298 ± 2 K	308 ± 2 K	328 ± 2 K	338 ± 2 K
$P_{CO_2}$ (Barrer)	SG	1.12 ± 0.05	1.39 ± 0.05	2.5 ± 0.1	3.2 ± 0.1
	M224	1.10 ± 0.05	1.35 ± 0.05	2.5 ± 0.1	3.1 ± 0.1
	M225	1.10 ± 0.05	1.37 ± 0.05	2.6 ± 0.1	3.1 ± 0.1
$P_{CO}$ (Barrer)	SG	0.07 ± 0.01	0.10 ± 0.01	0.24 ± 0.01	0.37 ± 0.02
	M224	0.09 ± 0.01	0.14 ± 0.01	0.28 ± 0.01	0.40 ± 0.02
	M225	0.08 ± 0.02	0.12 ± 0.02	0.25 ± 0.02	0.38 ± 0.02
$D_{CO_2}$ (cm <sup>2</sup> /s)	SG	$(4.0 \pm 0.2) \times 10^{-9}$	$(5.6 \pm 0.2) \times 10^{-9}$	$(1.68 \pm 0.06) \times 10^{-8}$	$(2.4 \pm 0.1) \times 10^{-8}$
	M224	$(3.8 \pm 0.2) \times 10^{-9}$	$(5.7 \pm 0.2) \times 10^{-9}$	$(1.60 \pm 0.06) \times 10^{-8}$	$(2.4 \pm 0.1) \times 10^{-8}$
	M225	$(3.8 \pm 0.2) \times 10^{-9}$	$(5.7 \pm 0.2) \times 10^{-9}$	$(1.62 \pm 0.06) \times 10^{-8}$	$(2.4 \pm 0.1) \times 10^{-8}$
$D_{CO}$ (cm <sup>2</sup> /s)	SG	$(9.2 \pm 0.4) \times 10^{-9}$	$(1.61 \pm 0.08) \times 10^{-8}$	$(5.4 \pm 0.2) \times 10^{-8}$	$(8.7 \pm 0.3) \times 10^{-8}$
	M224	$(1.00 \pm 0.04) \times 10^{-8}$	$(1.50 \pm 0.06) \times 10^{-8}$	$(5.2 \pm 0.2) \times 10^{-8}$	$(9.0 \pm 0.4) \times 10^{-8}$
	M225	$(9.7 \pm 0.6) \times 10^{-9}$	$(1.55 \pm 0.06) \times 10^{-8}$	$(5.1 \pm 0.2) \times 10^{-8}$	$(8.7 \pm 0.4) \times 10^{-8}$
$P_{O_2}$ (Barrer)	SG	0.29 ± 0.02	0.40 ± 0.02	0.73 ± 0.04	1.04 ± 0.04
	M224	0.30 ± 0.02	0.41 ± 0.02	0.70 ± 0.04	0.92 ± 0.05
	M225	0.30 ± 0.02	0.40 ± 0.03	0.71 ± 0.04	0.95 ± 0.05
$D_{O_2}$ (cm <sup>2</sup> /s)	SG	$(4.3 \pm 0.2) \times 10^{-8}$	$(6.0 \pm 0.2) \times 10^{-8}$	$(1.8 \pm 0.1) \times 10^{-7}$	$(2.5 \pm 0.1) \times 10^{-7}$
	M224	$(4.1 \pm 0.2) \times 10^{-8}$	$(7.1 \pm 0.2) \times 10^{-8}$	$(1.8 \pm 0.1) \times 10^{-7}$	$(2.4 \pm 0.1) \times 10^{-7}$
	M225	$(4.1 \pm 0.2) \times 10^{-8}$	$(7.0 \pm 0.2) \times 10^{-8}$	$(1.9 \pm 0.1) \times 10^{-7}$	$(2.3 \pm 0.1) \times 10^{-7}$
$P_{N_2}$ (Barrer)	SG	0.05 ± 0.01	0.07 ± 0.01	0.19 ± 0.01	0.26 ± 0.02
	M225	0.04 ± 0.01	0.06 ± 0.01	0.20 ± 0.02	0.26 ± 0.03
$D_{N_2}$ (cm <sup>2</sup> /s)	SG	$(7.1 \pm 0.4) \times 10^{-9}$	$(1.2 \pm 0.1) \times 10^{-8}$	$(4.0 \pm 0.2) \times 10^{-8}$	$(6.1 \pm 0.3) \times 10^{-8}$
	M225	$(7.0 \pm 0.3) \times 10^{-9}$	$(1.1 \pm 0.2) \times 10^{-8}$	$(4.0 \pm 0.3) \times 10^{-8}$	$(6.0 \pm 0.4) \times 10^{-8}$

696 Table S13: Permeability and diffusivity numerical values of  $CO_2$ ,  $O_2$ ,  $N_2$  and  $CO$  in the PLA membrane sample ( $p_{feed}$   
697 between 20 and 90 kPa).  
698



699  
700

Membrane sample	$P_{CO_2}$ (barrer)	$P_{CO_2}/P_{CO}$ (*)	$E_p^{CO_2}$ (kJ/mol)	$E_p^{CO}$ (kJ/mol)	Test conditions	Ref.
Matrimid®	$8.1 \pm 0.3$	$17 \pm 1$	$7.7 \pm 0.5$	$20.7 \pm 0.9$	SG	This work
PEI	$1.17 \pm 0.05$	$17 \pm 1$	$1.0 \pm 0.2$	$9.3 \pm 0.5$	SG	This work
PLA	$1.12 \pm 0.05$	$16 \pm 1$	$22.4 \pm 0.5$	$36 \pm 1$	SG	This work
Matrimid®	6.1	14	8.1	16.5	SG	[39]
Ultem® 1000	0.3	6	34.37	78.72	SG	[30]
PE (Grex)	0.36	1.87	30.15	39.37	SG	[40]
PE (Alathon)	12.63	8.50	38.95	46.49	SG	[40]
PE (Hydropol)	48.42	7.83	36.44	44.81	SG	[40]
Natural rubber	154	9.75	21.78	31	SG	[40]
PDMS	3200	6.4	2.2	11	GM (**)	[36]
PTMSP	18200	3.4	-6.5	-2.1	GM (**)	[36]
Pebax 2533	350	15.9	6.5	19.4	SG	[46]
Polyimide	1.48	22.7	12.8	23.4	SG	[43]

701

Table SI4

702

(\*)  $P_{CO_2}/P_{CO}$  values measured at near-ambient temperature.

703

SG: Single Gas

704

(\*\*) GM: Gas mixture 1.5 %  $H_2S$ , 10.5 %  $CO_2$ , 46%  $CO$  and 42 %  $H_2$

**Highlights:**

Gas mixtures produced by  $CO_2$  reforming processes.

$CO_2/CO$  separation by Matrimid®, polyetherimide and poly(lactic acid) membranes.

$CO$  and  $CO_2$  permeability/diffusivity obtained at different temperatures in single/mixed gas tests.

$CO_2/CO$  separation performances and mechanism analysed in ideal and mixed gas conditions.



Manuscript Number: MEMSCI-D-22-01187

Title: Mixed gas diffusion and permeation of ternary and quaternary CO<sub>2</sub>/CO/N<sub>2</sub>/O<sub>2</sub> gas mixtures in Matrimid®, polyetherimide and poly(lactic acid) membranes for CO<sub>2</sub>/CO separation.

By R. Checchetto et al.

#### **Author statement**

R. Checchetto: Conceptualization, methodology, investigation, writing.

M. G. De Angelis: Conceptualization, resources, writing.

M. Minelli: Conceptualization, resources, writing.

M. Scarpa: Conceptualization, resources, writing.

**Declaration of interests**

The authors declare that they have no known competing financial interests or personal relationships that could have appeared to influence the work reported in this paper.

The authors declare the following financial interests/personal relationships which may be considered as potential competing interests:

Journal Pre-proof